

for geotechnics & structures

---

# ELASTIC-PLASTIC DAMAGE MODEL FOR CONCRETE

**Report 020116**

(revised 02.01.2021)

**A. Truty**

**GeoDev.**

PO Box CH-1001 Lausanne  
Switzerland  
<https://zsoil.com>



# Contents

<b>1</b>	<b>Introduction</b>	<b>3</b>
<b>2</b>	<b>Reference plastic damage model for concrete (by Lee and Fenves) and its modifications</b>	<b>5</b>
2.1	Theory . . . . .	5
<b>3</b>	<b>Estimating model parameters</b>	<b>15</b>
3.1	Calibrating model parameters corresponding to the compressive stress domain	15
3.2	Calibrating model parameters corresponding to the tensile stress domain . . .	17
<b>4</b>	<b>Numerical implementation</b>	<b>19</b>
4.1	Stress strain integration scheme . . . . .	19
<b>5</b>	<b>Creep and aging</b>	<b>21</b>
5.1	Previous creep and aging implementation . . . . .	22
5.2	Aging and creep (edition 2020) . . . . .	24
<b>6</b>	<b>User interface</b>	<b>27</b>
<b>7</b>	<b>Benchmarks</b>	<b>31</b>
7.1	Gopalaratnam and Shah monotonic and cyclic uniaxial tensile tests (1985) .	31
7.2	Karsan and Jirsa monotonic and cyclic uniaxial compression tests (1969) . .	34
7.3	Kupfer's tests . . . . .	37
7.4	Three point bending test . . . . .	42
7.5	RC slab under point loading . . . . .	43
7.6	Creep in monotonic compression test . . . . .	47
7.7	Creep under variable loading conditions . . . . .	51
7.8	Creep under variable loading conditions at early stage of maturing . . . . .	52
7.9	Nonlinear monotonic creep compression test . . . . .	53



# Chapter 1

## Introduction

Current implementation of plastic damage model for concrete (CPDM) is based on the formulation proposed by Lee and Fenves [4, 5] including modifications of plastic flow potential introduced then by Omid and Lotfi [7] and important modifications proposed by the author of this report. This model couples single surface elasto-plasticity with hardening and an enhanced scalar damage allowing for description of stiffness degradation and stiffness recovery in cyclic tension-compression tests.



# Chapter 2

## Reference plastic damage model for concrete (by Lee and Fenves) and its modifications

### 2.1 Theory

In classical elastoplasticity, assuming that the linear elastic Hooke's law is used for the irreversible part of the deformation, the relation between stress and strain can be described in the following total form

$$\boldsymbol{\sigma} = \mathbf{E} : (\boldsymbol{\varepsilon} - \boldsymbol{\varepsilon}^p) \quad (2.1)$$

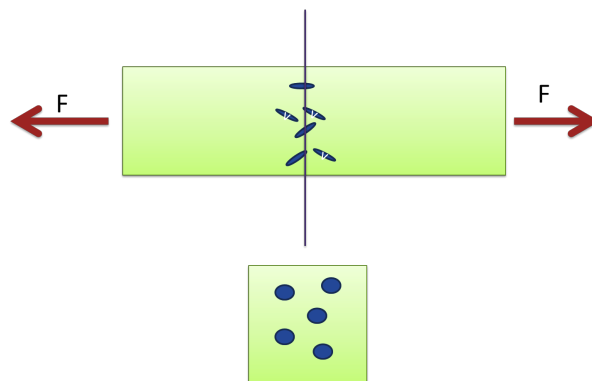


Figure 2.1: Damaged configuration (damaged cross section of a bar is shown below; dark dots represent here voids)

In the continuum damage theory notion of nominal and effective stresses is introduced (here effective stresses have nothing to do with the classical effective stresses known from mechanics of porous media) (see Fig.2.1). If we consider a 1D tensile test case then the corresponding nominal and effective axial stress can be defined as follows

$$\sigma = \frac{F}{A_o} \quad (2.2)$$

$$\bar{\sigma} = \frac{F}{A_o - A_{voids}} \quad (2.3)$$

In the general 2D or 3D problems the following mapping rule from nominal to the effective stress is used

$$\bar{\sigma} = \mathbf{D} : \sigma \quad (2.4)$$

where  $\mathbf{D}$  is the 4-th order mapping tensor (in general), and ":" symbol represents tensor product ( $\bar{\sigma}_{ij} = \mathbf{D}_{ijkl} \sigma_{kl}$ ). Effective stresses are always overlined (e.g.  $\bar{\sigma}$ , in matrix notation, or  $\bar{\sigma}_{ij}$ , in the tensorial one) in the report, while principal stresses (no matter if nominal or effective) are distinguished by an extra hat symbol (e.g.  $\hat{\sigma}_i$ , if nominal, or  $\hat{\bar{\sigma}}_i$ , if the effective principal stress is considered).

All major components of the CPDM model, basing on the assumption of strain equivalence in terms of the damage formulation, are summarized in Win.(2-1)

## Window 2-1: Major components of CPDM model

ZSoil<sup>®</sup>

- Mapping tensor  $\mathbf{D}$  in isotropic damage ( $\mathbf{I}$  is an unit tensor here while  $D$  is a damage parameter ( $0 \leq D \leq 1$ ))

$$\mathbf{D} = \frac{1}{1 - D} \mathbf{I}$$

- Relation between nominal and effective stresses

$$\boldsymbol{\sigma} = (1 - D) \bar{\boldsymbol{\sigma}}$$

- Constitutive equation written in terms of nominal stresses

$$\boldsymbol{\sigma} = (1 - D) \mathbf{E} : (\boldsymbol{\varepsilon} - \boldsymbol{\varepsilon}^p)$$

- Set of internal damage variables:  $\boldsymbol{\kappa} = \{\kappa_c, \kappa_t\}^\top$
- Evolution law for damage variables ( $\mathbf{H}$  is a diagonal matrix of hardening functions specified later on)

$$\dot{\boldsymbol{\kappa}} = \dot{\lambda} \mathbf{H}(\bar{\boldsymbol{\sigma}}, \boldsymbol{\kappa})$$

- Enhanced damage parameter (combination of two damage parameters corresponding to the compression  $D_c(\kappa_c)$  (see Win.(2-2)) and tension  $D_t(\kappa_t)$  (see Win.(2-4))

$$D = 1 - (1 - D_c(\kappa_c))(1 - s D_t(\kappa_t))$$

- Stiffness recovery function

$$s(\hat{\boldsymbol{\sigma}}) = s_o + (1 - s_o) r(\hat{\boldsymbol{\sigma}})$$

- Effective stress domain function

$$r(\hat{\boldsymbol{\sigma}}) = \frac{\sum_{i=1}^3 \langle \hat{\boldsymbol{\sigma}}_i \rangle}{\sum_{i=1}^3 |\hat{\boldsymbol{\sigma}}_i|}$$

- Plastic yield condition (see Win.(2-5))

$$F(\bar{\boldsymbol{\sigma}}, \boldsymbol{\kappa}) = 0$$

- Plastic flow rule ( $G$  is a modified Drucker-Prager type potential) (see Win.(2-6))

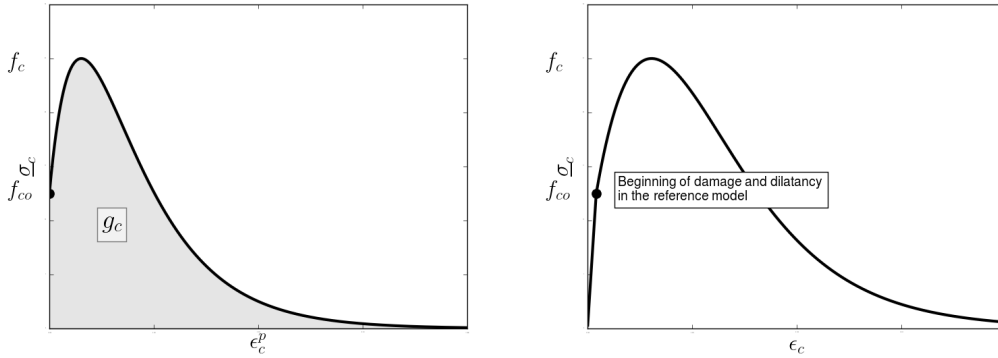
$$\dot{\boldsymbol{\varepsilon}}^p = \dot{\lambda} \frac{\partial G}{\partial \bar{\boldsymbol{\sigma}}}$$

Window 2-1

**Window 2-2: Internal damage variable  $\kappa_c$  in compression and damage factor  $D_c$**  ZSoil®

- Nominal compressive stress:  $\underline{\sigma}_c = \underline{f}_{co} [(1 + a_c) \exp(-b_c \varepsilon_c^p) - a_c \exp(-2 b_c \varepsilon_c^p)]$
- Normalized fracture energy:  $g_c = \frac{G_c}{l_c} = \int_0^\infty \underline{\sigma}_c(\varepsilon_c^p) d\varepsilon_c^p$
- Evolution law for hardening variable  $\varepsilon_c^p$ :  $\dot{\varepsilon}_c^p = -(1 - r(\hat{\sigma})) \dot{\varepsilon}_{min}^p$
- Internal damage variable:  $\kappa_c = \frac{1}{g_c} \int_0^{\varepsilon_c^p} \underline{\sigma}_c(\varepsilon_c^p) d\varepsilon_c^p$
- Evolution law for damage variable:  $\dot{\kappa}_c = \frac{1}{g_c} \underline{\sigma}_c(\kappa_c) \dot{\varepsilon}_c^p$

$$\kappa_c = 1 - \frac{\underline{f}_{co}}{g_c b_c} \left[ (1 + a_c) \exp(-b_c \varepsilon_c^p) - \frac{1}{2} a_c \exp(-2 b_c \varepsilon_c^p) \right]$$



Notion of normalized fracture energy  $g_c$  and uniaxial  $\sigma - \varepsilon$  diagram

- Damage parameter in compression:  $D_c = 1 - \exp(-d_c < \varepsilon_c^p - \varepsilon_{c,D}^p >)$
- Replacing hardening parameter  $\varepsilon_c^p$  by damage variable  $\kappa_c$  leads to the following expressions for  $\underline{\sigma}_c$  and  $D_c$  :

$$\underline{\sigma}_c(\kappa_c) = \frac{\underline{f}_{co}}{a_c} (1 + a_c - \sqrt{\phi_c}) \sqrt{\phi_c}$$

$$D_c = \begin{cases} 0 & \text{for } \kappa_c \leq \kappa_{c,D} \\ 1 - \left( \frac{1 + a_c - \sqrt{\phi_c}}{a_c x_1} \right)^{d_c/b_c} & \text{for } \kappa_c > \kappa_{c,D} \end{cases}$$

$$x_1 = \frac{1 + a_c - \sqrt{\phi_c(\kappa_{c,D})}}{a_c}$$

$$\phi_c(\kappa_c) = \frac{2 a_c b_c g_c (\kappa_c - 1)}{\underline{f}_{co}} + (1 + a_c)^2$$

- Effective compressive stress:

$$\bar{\sigma}_c(\kappa_c) = \begin{cases} \frac{\underline{f}_{co}}{a_c} \left( \frac{1 + a_c - \sqrt{\phi_c}}{a_c} \right) \sqrt{\phi_c} & \text{for } \kappa_c \leq \kappa_{c,D} \\ \frac{\underline{f}_{co}}{x_1^{-d_c/b_c}} \left( \frac{1 + a_c - \sqrt{\phi_c}}{a_c} \right)^{1-d_c/b_c} \sqrt{\phi_c} & \text{for } \kappa_c > \kappa_{c,D} \end{cases}$$

**Remarks**

1.  $\underline{f}_{co}$  is the initial compressive strength (according to the EC2  $\underline{f}_{co}/\underline{f}_c \approx 0.4$ )
2.  $\underline{\sigma}_{c,D}/\underline{f}_c$  can be assumed as  $\underline{\sigma}_{c,D}/\underline{f}_c = \frac{1}{\nu} \frac{f_t}{\underline{f}_c}$  (at this stress level the transverse normal strain reaches value  $f_t/E$ ); in the reference model  $\varepsilon_{c,D}^p = 0$  ( $\underline{\sigma}_{c,D}/\underline{f}_c = \underline{f}_{co}/\underline{f}_c$ )
3.  $\kappa_{c,D}$  is the damage variable that corresponds to the stress level  $\underline{\sigma}_{c,D}/\underline{f}_c$  in the uniaxial compression test
4.  $a_c$ ,  $b_c$  and  $d_c$  are material properties (see Win.(3-1) and Win.(3-2) for details concerning their calibration)
5. the characteristic length  $l_c$  is equal to the size of the finite element  $h_e$
6.  $\underline{\varepsilon}_c^p$  corresponds is the largest compressive plastic strain

Window 2-2

**Window 2-3: Determining value of damage variable  $\kappa_c$  for given stress level**

ZSoil®

- To determine value of damage variable  $\kappa_c$  for a given stress level in the uniaxial compression test we may use the equation

$$\underline{\sigma}_c(\kappa_c) = \frac{\underline{f}_{co}}{a_c} (1 + a_c - \sqrt{\phi_c}) \sqrt{\phi_c}$$

- Its nondimensional form is as follows

$$\frac{\underline{\sigma}_c}{\underline{f}_c} = \frac{\underline{f}_{co}}{\underline{f}_c a_c} (1 + a_c - \sqrt{\phi_c}) \sqrt{\phi_c}$$

- In the pre-peak zone one can compute  $\sqrt{\phi_c}$  value for a given stress level  $\frac{\underline{\sigma}_c}{\underline{f}_c}$  as follows

$$\sqrt{\phi_c} = \frac{\underline{f}_{co}(1 + a_c) - \sqrt{\Delta} \underline{f}_c a_c}{2 \underline{f}_{co}}$$

- In the post-peak zone

$$\sqrt{\phi_c} = \frac{\underline{f}_{co}(1 + a_c) + \sqrt{\Delta} \underline{f}_c a_c}{2 \underline{f}_{co}}$$

- $\Delta = \left( \frac{\underline{f}_{co}(1 + a_c)}{\underline{f}_c a_c} \right)^2 - 4 \frac{\underline{f}_{co}}{\underline{f}_c a_c} \frac{\underline{\sigma}_c}{\underline{f}_c}$

## CHAPTER 2. REFERENCE PLASTIC DAMAGE MODEL FOR CONCRETE (BY LEE AND FENVES) AND ITS MODIFICATIONS

---

- Then for given  $\sqrt{\phi_c}$  one may compute  $\kappa_c$  value using the following formula

$$\kappa_c = \frac{f_{co} (\phi_c - (1 + a_c)^2)}{2 a_c b_c g_c} + 1$$

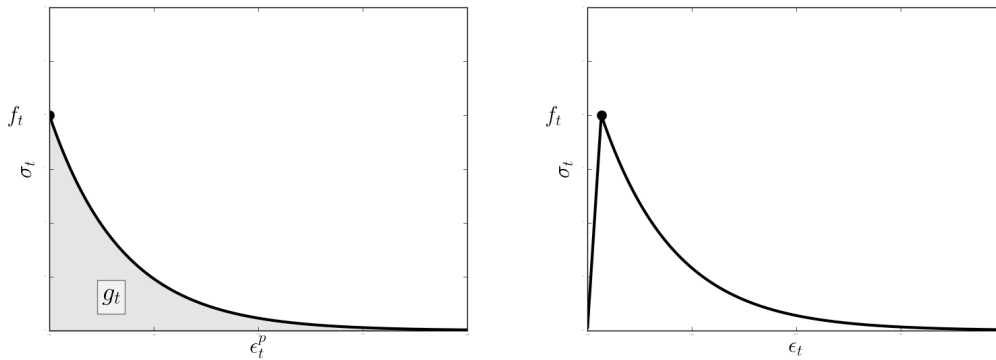
---

Window 2-3
------------

<b>Window 2-4: Internal damage variable <math>\kappa_t</math> in tension and damage factor <math>D_t</math></b>
---

ZSoil®

- Nominal tensile stress:  $\sigma_t = f_{to} [(1 + a_t) \exp(-b_t \varepsilon_t^p) - a_t \exp(-2 b_t \varepsilon_t^p)]$
- Here we assume:  $a_t = 0$
- Normalized fracture energy:  $g_t = \frac{G_t}{l_c} = \int_0^{\infty} \sigma_t(\varepsilon_t^p) d\varepsilon_t^p$
- Internal damage variable:  $\kappa_t = \frac{1}{g_t} \int_0^{\varepsilon_t^p} \sigma_t(\varepsilon_t^p) d\varepsilon_t^p = \frac{f_{to}}{g_t b_t} (1 - \exp(-b_t \varepsilon_t^p))$
- Evolution law for the hardening variable  $\varepsilon_t^p$ :  $\dot{\varepsilon}_t^p = r(\hat{\sigma}) \dot{\varepsilon}_{max}^p$
- Evolution law for damage variable:  $\dot{\kappa}_t = \frac{1}{g_t} \sigma_t(\kappa_t) \dot{\varepsilon}_t^p$

Notion of normalized fracture energy  $g_t$  and uniaxial  $\sigma - \varepsilon$  diagram

- Damage factor in tension:  $D_t = 1 - \exp(-d_t \varepsilon_t^p)$
- Replacing hardening parameter  $\varepsilon_t^p$  by  $\kappa_t$  yields the following expressions for  $\sigma_t$  and  $D_t$ 

$$\sigma_t(\kappa_t) = f_{to}(1 - \kappa_t)$$

$$D_t = 1 - (1 - \kappa_t)^{d_t/b_t}$$
- Effective tensile stress:  $\bar{\sigma}_t(\kappa_t) = f_{to} (1 - \kappa_t)^{1-d_t/b_t}$

**Remarks**

1.  $\varepsilon_t^p$  is the largest positive principal plastic strain

Window 2-4
------------

**Window 2-5: Plastic yield condition**

ZSoil®

- Yield condition (reference model ( $\rho = 0$ )):

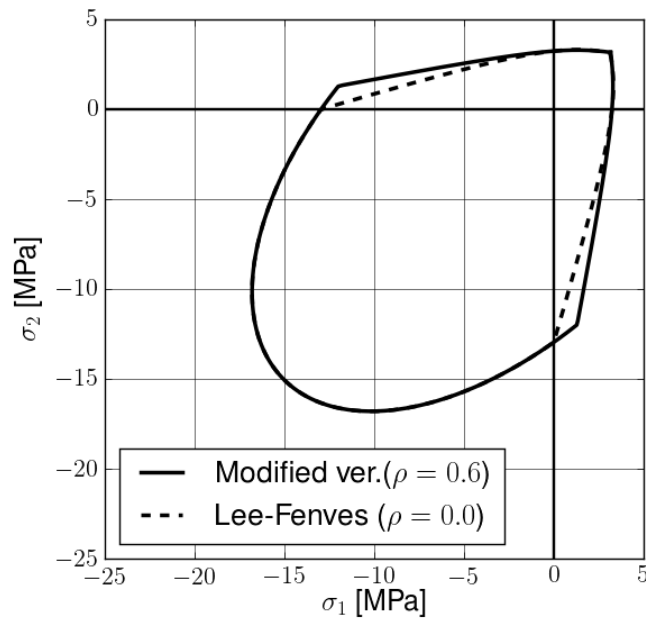
$$F(\bar{\sigma}, \kappa_t, \kappa_c) = \frac{1}{1 - \alpha} \left( \alpha I_1 + \sqrt{3} J_2 + \beta(\kappa_t, \kappa_c) \langle \hat{\sigma}_{max} \rangle \right) - c_c(\kappa_c)$$

$$\star \beta = \frac{c_c(\kappa_c)}{c_t(\kappa_t)} (1 - \alpha) - (1 + \alpha)$$

$$\star c_c = \bar{c}_c(\kappa_c) \quad c_t = \bar{c}_t(\kappa_t)$$

- Yield condition (modified version ( $\rho = 0.6$ )):

$$F(\bar{\sigma}, \kappa_t, \kappa_c) = \frac{1}{1 - \alpha} \left( \alpha I_1 + \sqrt{3} J_2 + \frac{\beta(\kappa_t, \kappa_c)}{1 - \rho} \langle \hat{\sigma}_{max} - \rho c_t \rangle \right) - c_c(\kappa_c)$$



Initial strength envelopes for reference and modified models

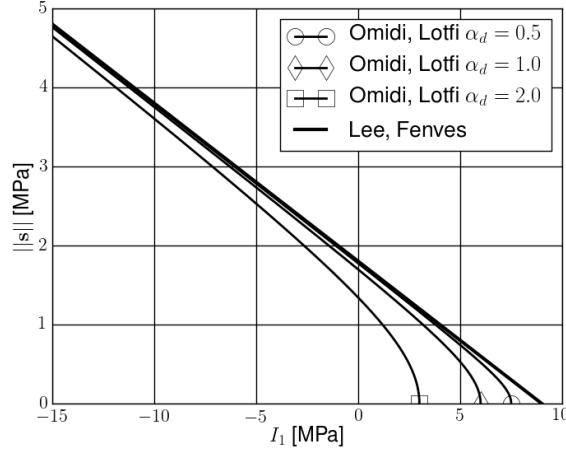
**Remarks**

1. In the mixed tension-compression tests (Kupfer tests) reference model may undershoot the ultimate compressive stress by more than 40 %; the introduced modification (via  $\rho = 0.6$  parameter) cancels this parasitic effect

Window 2-5

**Window 2-6: Plastic flow rule and evolution laws for plastic hardening variables  $\varepsilon_t^p$ ,  $\varepsilon_c^p$** 

ZSoil®

Smoothed plastic flow potential in  $I_1 - \sqrt{J_2}$  plane

- Plastic flow potential:  $G(\bar{\sigma}) = \sqrt{2 J_2 + \beta_H^2} + \alpha_p^* I_1$
- Constant dilatancy:  $\alpha_p^* = \alpha_p$
- Variable dilatancy:  $\alpha_p^* = \alpha_{po} f_{\kappa_t}(\kappa_t) + (1 - f_{\kappa_t}(\kappa_t)) f_{\kappa_c}(\kappa_c) \alpha_p$ 
  - ★  $f_{\kappa_t}(\kappa_t) = \begin{cases} \frac{3}{2}\bar{\kappa}_t - \frac{1}{2}\bar{\kappa}_t^3 & \text{for } \bar{\kappa}_t \leq 1 \\ 1 & \text{for } \bar{\kappa}_t > 1 \end{cases}$
  - ★  $\bar{\kappa}_t = \frac{\kappa_t}{\kappa_{t,ref}} \quad (\kappa_{t,ref} = 0.1)$
  - ★  $f_{\kappa_c}(\kappa_c) = \begin{cases} 0 & \text{for } \bar{\kappa}_c \leq 0 \\ 3\bar{\kappa}_c^2 - 2\bar{\kappa}_c^3 & \text{for } 0 \leq \bar{\kappa}_c \leq 1 \\ 1 & \text{for } \bar{\kappa}_c > 1 \end{cases}$
  - ★  $\bar{\kappa}_c = \frac{\kappa_c - \kappa_{c,dil}}{\kappa_{c,peak} - \kappa_{c,dil}}$
- Smoothing factor that cancels apex effect:  $\beta_H = \alpha_d f_t \alpha_{po}$

**Remarks**

1. Omid and Lotfi [7] added the term  $\beta_H$  to the plastic flow potential; this trick helps to avoid apex state that may appear in the standard Drucker-Prager plastic flow potential used by Lee and Fenves;  $\alpha_d = 1.0$  seems to be a reasonable value of this smoothing parameter
2.  $\kappa_{c,dil}$  and  $\kappa_{c,peak}$  are damage variables corresponding to the stress levels  $\underline{\sigma}_{c,dil}/\underline{f}_c$  and 1, respectively, in the uniaxial compression test (see Win.(2-3))
3. In the extended version dilatancy may vary with plastic straining; its value is kept zero till  $\kappa_c = \kappa_{c,dil}$  and then it grows up till  $\alpha_p$  value at  $\kappa_c = \kappa_{c,peak}$  (here a spline function is used)

Window 2-6



# Chapter 3

## Estimating model parameters

### 3.1 Calibrating model parameters corresponding to the compressive stress domain

Window 3-1: Estimation of  $a_c$  parameter

---

ZSoil®

- The general expression for the current compressive strength:

$$\underline{\sigma}_c = \underline{f}_{co} [(1 + a_c) \exp(-b_c \varepsilon_c^p) - a_c \exp(-2 b_c \varepsilon_c^p)]$$

- Let us assume that the peak compressive strength is equal to  $\max(\underline{\sigma}_c) = \underline{f}_c$

- The extremum of  $\underline{\sigma}_c$  is achieved at  $\varepsilon_{c,extr}^p = -\frac{\ln\left(\frac{1}{2} \frac{1 + a_c}{a_c}\right)}{b_c}$

- If we substitute  $\varepsilon_{c,extr}^p$  to the expression for  $\underline{\sigma}_c$  we will obtain the relation:

$$\underline{f}_c = \frac{1}{4} \frac{\underline{f}_{co} (1 + a_c)^2}{a_c}$$

- From the above expression one may derive  $a_c$  as:

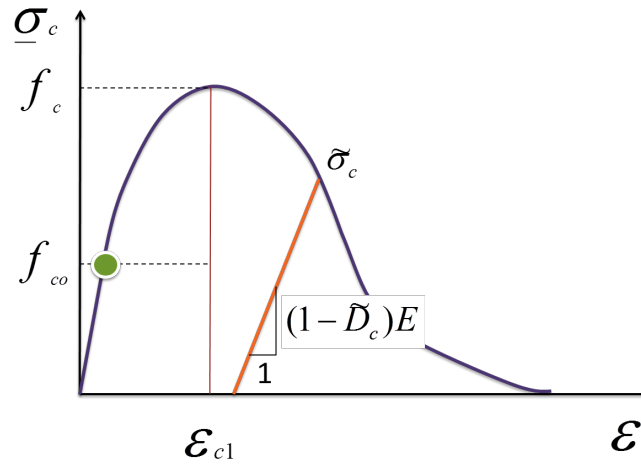
$$a_c = 2 \underline{f}_c / \underline{f}_{co} - 1 + 2 \sqrt{(\underline{f}_c / \underline{f}_{co})^2 - \underline{f}_c / \underline{f}_{co}}$$

---

Window 3-1

**Window 3-2: Estimation of  $b_c$  and  $d_c$ : approach that preserves  $G_c$  and  $\tilde{D}_c$**

ZSoil®



- In this procedure we want to preserve
  - ★ normalized fracture energy  $g_c = G_c/l_c$  value
  - ★ given damage factor  $\tilde{D}_c$  at a given stress  $\tilde{\sigma}_c$
- Using the expression for normalized fracture energy in compression one may easily derive value of  $b_c$  parameter
 
$$b_c = \frac{f_{co} (1 + a_c/2)}{g_c}$$
- Then the  $d_c$  parameter is computed as
 
$$d_c = b_c \frac{\ln(1 - \tilde{D}_c)}{\ln\left(\frac{1 + a_c - \sqrt{\phi_c^*}}{x_1 a_c}\right)}$$

the  $\phi_c^*$  value corresponds to the stress level value  $\tilde{\sigma}_c/f_c$  (use solution for the post-peak zone from Win.(2-3))

**Remarks**

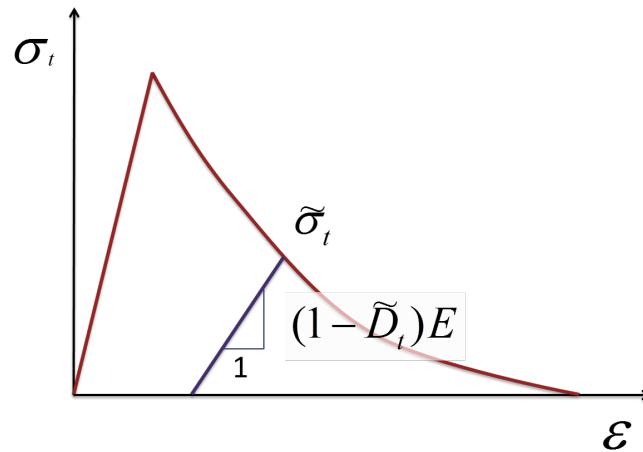
1. Strain at peak  $\varepsilon_{c1}$  is not under control
2. For assumed  $\sigma_{c,D}/f_c$  value the  $\tilde{D}_c$  is constrained by the condition  $d_c \geq b_c$ ; for decreasing values of  $\tilde{D}_c$  the  $\sigma_{c,D}/f_c$  value becomes larger, and vice versa (this limit condition is controlled in the user interface)

Window 3-2

### 3.2 Calibrating model parameters corresponding to the tensile stress domain

Window 3-3: Estimation of  $b_t$  and  $d_t$

ZSoil®



- Once the normalized fracture energy  $g_t$  is known one may derive  $b_t$  parameter:

$$b_t = \frac{f_{to}}{g_t}$$

- Here for given stress value  $\tilde{\sigma}_t$  damage factor in tension is known and equal to  $\tilde{D}_t$

- Plastic tensile strain corresponding to the stress value  $\tilde{\sigma}_t$  is equal to

$$\tilde{\epsilon}_t^p = -\frac{\ln(\tilde{\sigma}_t/f_{to})}{b_t}$$

- $d_t$  parameter is equal to

$$d_t = -\frac{\ln(1 - \tilde{D}_t)}{\tilde{\epsilon}_t^p}$$

Window 3-3

**Window 3-4: Directional element size  $h_e$** 

ZSoil®

- Directional element size is defined as follows:

$$h_e = r(\hat{\sigma}_i) h_e^{\varepsilon_1} + (1 - r(\hat{\sigma}_i)) h_e^{\varepsilon_3}$$

- $h_e^{\varepsilon_1}$  is the element size measured along direction of  $\varepsilon_1$
- $h_e^{\varepsilon_3}$  is the element size measured along direction of  $\varepsilon_3$
- Element size in the direction of a given unit vector  $\mathbf{v}$  is defined as follows

$$h_e = \sum_{i=1}^{Ndm} h_{\xi_i} \left( \frac{v_{\xi_i}}{\|\mathbf{v}\|} \right)^2$$

$$h_i^{(\xi)} = \left\| \mathbf{x} \left( \mathbf{A}_{\xi_i}^{(+)} \right) - \mathbf{x} \left( \mathbf{A}_{\xi_i}^{(-)} \right) \right\|$$

where

$$\begin{aligned} \left( \mathbf{A}_{\xi_i}^{(+)} \right)_k &= \delta_{ki}, & \left( \mathbf{A}_{\xi_i}^{(-)} \right)_k &= -\delta_{ki}, & \mathbf{v}_{\xi}^T &= \mathbf{J}^{-1} \mathbf{v}^T, \\ \xi_1 &= \xi, & \xi_2 &= \eta, & \xi_3 &= \zeta \end{aligned}$$

and  $\mathbf{J}$  is the Jacobian matrix of the isoparametric mapping,  $v_{\xi_i}$  is the  $i$ -th component of a given vector in the local  $(\xi, \eta, \zeta)$  coordinate system,  $\delta_{ki}$  is the Kronecker's symbol,  $\mathbf{A}_{\xi_i}^{(+)}$  and  $\mathbf{A}_{\xi_i}^{(-)}$  are points with  $Ndm$  coordinates defined in the local system. The geometrical interpretation of this definition is shown in Fig. 1.

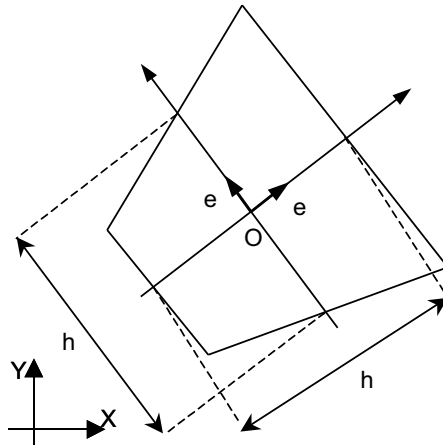


Figure 1: Definition (D2) for element Q4

**Remarks**

1. In the current implementation element size is kept constant within the given time step and based on the total strain tensor set up at the previous converged step (explicit scheme)

Window 3-4

# Chapter 4

## Numerical implementation

The stress-strain integration procedure of the modified Lee-Fenves model was developed in the principal stress space following the the scheme proposed by Runesson and Larson. This scheme can be adopted here as the principal effective stress directions become unchanged during plastic correction. This is caused by the conical form of the plastic potential.

### 4.1 Stress strain integration scheme

#### Window 4-1: General scheme

ZSoil<sup>®</sup>

- Transform nominal stress state at the last converged step  $N$  to the effective stress state

$$\bar{\sigma}_N = \frac{1}{1 - D_N} \sigma_N$$

- Compute trial effective stress state:

$$\bar{\sigma}_{N+1}^{\text{tr}} = \bar{\sigma}_N + \bar{D}^e \Delta \epsilon_{N+1}$$

- Compute principal effective stress state:  $\hat{\sigma}_{N+1}$

- Set initial values of damage variables:

$$\kappa_{t,N+1} = \kappa_{t,N}$$

$$\kappa_{c,N+1} = \kappa_{c,N}$$

- If  $F(\hat{\sigma}_{N+1}, \kappa_{t,N}, \kappa_{c,N}) \geq 0$ : perform plastic corrector algorithm (Win.(4-2))

- If  $F(\hat{\sigma}_{N+1}, \kappa_{t,N}, \kappa_{c,N}) < 0$ : update current stress state:  $\bar{\sigma}_{N+1} = \bar{\sigma}_{N+1}^{\text{tr}}$

- Update damage parametr:  $D_{N+1}$

- Map current effective stress to the nominal stress state:

$$\bar{\sigma}_{N+1} = (1 - D_{N+1}) \sigma_{N+1}$$

Window 4-1

**Window 4-2: Plastic corrector algorithm**

ZSoil®

Set of independent variables:  $\{\Delta\hat{\varepsilon}_{N+1}^p, \kappa_{t,N+1}, \kappa_{c,N+1}, \Delta\lambda_{N+1}\}^T$

Stress-strain integration is carried out by solving the following set of nonlinear equations

1.  $\mathbf{r}_{\varepsilon^p} = \Delta\hat{\varepsilon}_{N+1}^p - \Delta\lambda_{N+1} \mathbf{b}(\hat{\boldsymbol{\sigma}}_{N+1}, \kappa_{t,N+1}, \kappa_{c,N+1}) = 0$
2.  $\mathbf{r}_{\kappa_t} = \kappa_{t,N+1} - \kappa_{t,N} - \frac{\sigma_t(\kappa_{t,N+1})}{g_t} r(\hat{\boldsymbol{\sigma}}_{N+1}) < \Delta\varepsilon_1^p > = 0$
3.  $\mathbf{r}_{\kappa_c} = \kappa_{c,N+1} - \kappa_{c,N} - \frac{\sigma_c(\kappa_{c,N+1})}{g_c} (1 - r(\hat{\boldsymbol{\sigma}}_{N+1})) < -\Delta\varepsilon_3^p > = 0$
4.  $\mathbf{r}_F = F(\hat{\boldsymbol{\sigma}}_{N+1}, \kappa_{t,N+1}, \kappa_{c,N+1}) = 0$

This system is solved using an iterative Newton-Raphson scheme.

Window 4-2

# Chapter 5

## Creep and aging

The implemented model can also describe a visco-elastic aging creep phenomenon following the EC2 standard (EN 1992-1-1:2004+AC:2008). Nonlinear creep effects that may appear for larger compressive stresses are automatically included once the onset of damage is set at stress level  $\sigma_c/f_c \approx 0.4$ . The resulting creep amplification in compression will be of order  $1/(1 - \tilde{D}_c)$  ( $\tilde{D}_c$  is set at the peak).

**It has to be emphasized that creep is induced by the stress change in general. Therefore if the structure exists let say since time  $t_o$  but creep is activated later on at time  $t_1$ , and  $t_1 > t_o$ , then the preexisting stress state before time  $t_1$  will not influence evolution of creep strains. In this case creep strains will be driven by the stress change  $\Delta\sigma = \sigma - \sigma(t_o)$ .**

### Window 5-1: Description of creep phenomenon in the EC2

ZSoil®

• Time dependent creep coefficient:  $\phi(t, t_o) = \phi_o \beta_c(t, t_o)$

• Basic creep coefficient:  $\phi_o = \phi_{RH} \beta(f_{cm}) \beta(t_o)$

$$\bullet \phi_{RH} = \begin{cases} 1 + \frac{1 - \frac{RH}{100}}{0.1 h_o^{1/3}} & \text{for } f_{cm} \leq 35 \text{ MPa} \\ \left( 1 + \frac{1 - \frac{RH}{100}}{0.1 h_o^{1/3}} \alpha_1 \right) \alpha_2 & \text{for } f_{cm} > 35 \text{ MPa} \end{cases}$$

$$\bullet \beta(f_{cm}) = \frac{16.8}{\sqrt{f_{cm}}}$$

$$\bullet \beta(t_o) = \frac{1}{0.1 + t_o^{0.2}}$$

$$\bullet \beta_c(t, t_o) = \left[ \frac{t - t_o}{\beta_H + t - t_o} \right]^{0.3}$$

$$\bullet \beta_H = \begin{cases} \min(1.5 [1 + (0.012RH)^{18}] h_o + 250, 1500) & \text{for } f_{cm} \leq 35 \text{ MPa} \\ \min(1.5 [1 + (0.012RH)^{18}] h_o + 250\alpha_3, 1500\alpha_3) & \text{for } f_{cm} > 35 \text{ MPa} \end{cases}$$

**Remarks:**

1. Creep coefficient is understood as a ratio between creep strain  $\varepsilon^{cr}$  and an instantaneous elastic strain computed for concrete loaded at  $t = 28$  days
2. In the above expressions  $\alpha_1 = (35/f_{cm})^{0.7}$ ,  $\alpha_2 = (35/f_{cm})^{0.2}$ ,  $\alpha_3 = (35/f_{cm})^{0.5}$ , relative humidity  $RH$  is expressed in [%], the equivalent member size  $h_o$  is expressed in [mm], an averaged compressive strength  $f_{cm}$  is expressed in [MPa] and loading time  $t_o$  is expressed in [days]
3. Time parameter  $t$  and  $t_o$  can be replaced by a corresponding temperature adjusted value  $t_T$  defined as follows

$$t_T(t) = \int_{t_1}^t \exp\left(-\frac{Q}{R} \left( \frac{1}{273 + T(\tau)} - \frac{1}{273 + T_{ref}} \right)\right) d\tau$$

( $T_{ref} = 20$  [°C])

Window 5-1

## 5.1 Previous creep and aging implementation

The creep and aging module developed for the damage model in previous ZSoil versions (since 2016) enabled one to consider rheological effects in concrete assuming that the duration of breaks between loading phases was not too big. For the sake of back compatibility this implementation can still be used, however, using the new one is highly recommended. The new implementation will be called as edition 2020. The previous implementation will be obsolete in the future ZSoil versions.

**Window 5-2: Implementation of the previous EC2 visco-elastic creep**

ZSoil®

Implementation scheme is partially based on algorithm proposed by Havlásek [1]. The main goal in the implementation scheme is to avoid time dependent values of  $A_\mu$  parameters. Therefore current creep strain increment is divided by the  $v^{cr}$  factor that amplifies (in early stages) or reduces (for old concrete) creep rate. In this approach the experimental creep curve is approximated by a chain of nonaging Kelvin units.

- Creep strain increment is computed using the following scheme

$$\Delta\varepsilon_{n+1}^{cr} = \mathbf{D}_o^{-1} \frac{1}{v_{n+1/2}^{cr}} \sum_{\mu=1}^N A_\mu (1 - \beta_{\mu,n+1}) \boldsymbol{\sigma}_{v\mu,n}$$

where:

- ★  $\mathbf{D}_o^{-1}$  is an elastic compliance matrix computed for unit Young's modulus
- ★  $v_{n+1/2}^{cr}$  is an extra scaling factor amplifying creep rate due to aging phenomenon (here it is not equivalent to the fraction of solidified layers)
- ★  $\boldsymbol{\sigma}_{v\mu,n+1}$  represents viscous effective stresses in  $\mu - th$  Kelvin unit (number of Kelvin units in chain is denoted by  $N$ )

- ★  $\beta_{\mu,n+1} = \exp(-\Delta t_{n+1}/\tau_{\mu})$
- ★  $\tau_{\mu}$  is a retardation time of  $\mu$ -th Kelvin unit
- ★  $A_{\mu}$  is the ultimate creep strain value in  $\mu$ -th Kelvin unit
- Viscous stress update:  $\sigma_{v\mu,n+1} = \beta_{\mu,n+1}\sigma_{v\mu,n} + \lambda_{\mu,n+1}\Delta\bar{\sigma}_{n+1}$
- $\lambda_{\mu,n+1} = (1 - \beta_{\mu,n+1})\frac{\tau_{\mu}}{\Delta t_{n+1}}$
- The algorithmic effective Young's modulus is expressed as follows
 
$$\bar{E} = \frac{1}{\frac{1}{v^E E_{28}} + \frac{1}{v^{cr}} \sum_{\mu=1}^N (1 - \lambda_{\mu,n+1}) A_{\mu}}$$
- $v^E = \sqrt{\beta_{cc}}$
- $\beta_{cc} = \begin{cases} \exp(s(1 - \sqrt{28/t})) & \text{for } t \leq 28 \text{ days} \\ 1 & \text{for } t > 28 \text{ days} \end{cases}$

Window 5-2

**Window 5-3: Derivation of  $v^{cr}$  function**

ZSoil®

- Evolution of creep strain in time, according to EC2, can be expressed by the following equation
 
$$\varepsilon^{cr} = A_1 \left( \frac{t - t_o}{\beta_H + t - t_o} \right)^{0.3} \beta(t_o)$$
 where  $A_1 = \phi_{RH}\beta(f_{cm})/E$
- Evolution of the reference creep strain for concrete loaded at  $t_o = 28$  days (matured concrete) can be defined as
 
$$\varepsilon_{ref}^{cr} = A_1 \left( \frac{t - t_o}{\beta_H + t - t_o} \right)^{0.3} \beta(t_o = 28)$$
- The reference creep strain curve is taken here as a basis for optimization of  $A_{\mu}$  coefficients in chain of nonaging Kelvin units (retardation times  $\tau_{\mu}$  are predefined by considering duration of carried out analysis time)
- To derive  $v^{cr}$  we assume the following creep strain rates compatibility condition
 
$$\dot{\varepsilon}^{cr} = \frac{1}{v^{cr}} \dot{\varepsilon}_{ref}^{cr}$$
- This yields the following definition of  $v^{cr}$  function
 
$$v^{cr} = \frac{\beta(t_o = 28)}{\beta(t_o)}$$
 where  $t_o$  is the age of concrete at the beginning of analysis

Window 5-3

## 5.2 Aging and creep (edition 2020)

As it has been already mentioned application of the previous creep and aging module within the damage model was limited to the case when breaks in loading phases were not too long. In order to remedy this limitation a new implementation scheme was elaborated starting from the strict definition of the pure creep measure  $C(t, \tau)$ , compliance function  $\delta(t, \tau)$  and integral equation for the stress state tracing whole loading history. In the pure creep measure and in the compliance functions all EC2 creep and aging analytical functions are included.

### Window 5-4: EC2 based visco-elastic creep and aging (edition 2020)

ZSoil®

- Pure creep measure definition:  $C(t, \tau) = \tilde{\beta}_o \sum_{i=1}^N A_i (1 - e^{-\gamma_i(t-\tau)})$ 
  - ★  $C(t, \tau)$  expresses evolution of creep strain caused by the unit stress
  - ★  $N$  - number of Kelvin elements in chain approximating assumed analytical creep curve
  - ★  $\sum_{i=1}^N A_i (1 - e^{-\gamma_i(t-\tau)}) \approx \frac{\phi_{RH} \beta(f_{cm})}{E} \left( \frac{t - t_o}{\beta_H + t - t_o} \right)^{0.3} \beta(t_o = 28)$  - Kelvin chain approximation of the analytical creep strain evolution caused by the unit stress at age of  $t_o = 28$  days
  - ★  $\tilde{\beta}_o = \frac{\beta_o(\tau)}{\beta_o(t = 28)}$
  - ★  $\beta_o(\dots)$  function is equivalent to the EC2  $\beta(t_o)$  one
- Compliance function definition:  $\delta(t, \tau) = \frac{1}{E(\tau)} + C(t, \tau)$
- Integrated stress state:  $\sigma(t) = \mathbf{D}^e(t) \left( \boldsymbol{\varepsilon}(t) - \boldsymbol{\varepsilon}_o(t) - \int_{t_o}^t -\frac{\partial \delta(t, \tau)}{\partial \tau} \right)$
- Stress state:  $\sigma_n = \mathbf{D}_n^e \left( \boldsymbol{\varepsilon}_n - \boldsymbol{\varepsilon}_{o,n} - \int_{t_o}^{t_n} -\frac{\partial \delta(t_n, \tau)}{\partial \tau} \right)$
- Stress state:  $\sigma_{n-1} = \mathbf{D}_{n-1}^e \left( \boldsymbol{\varepsilon}_{n-1} - \boldsymbol{\varepsilon}_{o,n-1} - \int_{t_o}^{t_{n-1}} -\frac{\partial \delta(t_{n-1}, \tau)}{\partial \tau} \right)$
- Stress increment:  $\Delta \sigma_n = \sigma_n - \sigma_{n-1}$

Window 5-4

**Window 5-5: Recursive formula to compute creep strain increment (edition 2020)**

ZSoil®

Based on the stress increment  $\Delta\sigma_n$  defined in Win.5-5 one can derive the following recursive formula to compute increment of creep strains

- the full formula including predictor and corrector parts is expressed as follows

$$\begin{aligned}\Delta\epsilon_n^c &= \sum_{i=1}^N (e^{-\gamma_i\Delta t} - 1) \epsilon_{n-1}^{c,i} + \\ &+ (\sigma_{n-1} + \theta\Delta\sigma_n) \sum_{i=1}^N A_i \underbrace{\left( \tilde{\beta}_n - \tilde{\beta}_{n-1} e^{-\gamma_i\Delta t} \right)}_{\Delta w_{1,i}} + \\ &+ (\sigma_{n-1} + \theta\Delta\sigma_n) \sum_{i=1}^N A_i \underbrace{\left( -\tilde{\beta}_n + \tilde{\beta}_{n-1} \right)}_{\Delta w_{2,i}}\end{aligned}$$

- the creep strain predictor is extracted from the above expression

$$\Delta\epsilon_n^{c,\text{pred}} = \sum_{i=1}^N (e^{-\gamma_i\Delta t} - 1) \epsilon_{n-1}^{c,i} + \sigma_{n-1} \sum_{i=1}^N \Delta w_{1,i} + \sigma_{n-1} \sum_{i=1}^N \Delta w_{2,i}$$

- The algorithmic effective Young's modulus at step  $n$  is defined as

$$\bar{E}_n = \frac{E_n}{1 + \theta \frac{E_n - E_{n-1}}{E_{n-1}} + \theta E_n \sum_{i=1}^N (\Delta w_{1,i} + \Delta w_{2,i})}$$

Window 5-5



# Chapter 6

## User interface

**Window 6-1: Properties specific to concrete plastic damage model**

ZSoil®

Subgroup	Parameter	Unit	Range	Description
Strength in compression	$\underline{f}_c$	[MPa]		Uniaxial compressive strength; positive in compression; use according to standards (EC2 for instance)
	$\underline{f}_{co}/\underline{f}_c$	[-]	0.4÷0.8	Initial to peak compressive strength ratio
	$\underline{f}_{cbo}/\underline{f}_{co}$	[-]	1.1÷1.2	Initial biaxial to uniaxial strength ratio
Damage in compression	$\underline{\sigma}_{c,D}/\underline{f}_c$	[-]	0.4÷0.9	Stress level at which damage starts to occur; $\underline{\sigma}_{c,D}/\underline{f}_c \geq \underline{f}_{co}/\underline{f}_c$
	$\tilde{\sigma}_c/f_c$	[-]	$\leq 1.0$	Stress level for damage calibration (post-peak)
	$\tilde{D}_c$	[-]	$\geq 0.3$	Damage parameter in uniaxial compression at the assumed reference stress level; if this value is too small a warning will be generated
	$G_c$	[MN/m]	$50 G_t \leq G_c \leq 100 G_t$	Fracture energy in compression;
Strength in tension	$f_t$	[MPa]		Uniaxial tensile strength; positive in tension; use according to standards (EC2 for instance)
Damage in tension	$\tilde{\sigma}_t/f_t$	[-]	0.5 (< 1)	Stress level for damage calibration (post-peak)

	$\tilde{D}_t$	[-]	$\geq 0.3$	Damage parameter in uniaxial tension at the assumed reference stress level; if this value is too small a warning will be generated
	$G_t$	[MN/m]	$50 \cdot 10^{-6} \div 150 \cdot 10^{-6}$	Fracture energy in tension; can be estimated as $73 f_c^{0.18} \cdot 10^{-6}$ (use MPa as strength unit here)
	$s$	[-]	$0.1 \div 0.3$	Stiffness recovery factor due to crack closure for tension-compression cycles
Dilatancy	type		Constant/Variable	Dilatancy type
	$\alpha_p$	[-]	$0.1 \div 0.5$	Dilatancy parameter value for Constant option or dilatancy parameter in uniaxial compression when option Variable is used
	$\alpha_{po}$	[-]	$0.1 \div 0.4$	Dilatancy parameter in uniaxial tension option Variable is used
	$\underline{\sigma}_{c,dil}/\underline{f}_c$	[-]	$0.4 \div 1.0$	Activation of dilatancy in compression when Variable option is used; $\underline{\sigma}_{c,dil}/\underline{f}_c \geq \underline{f}_{co}/\underline{f}_c$
	$\alpha_d$	[-]	$0.2 \div 2.0$	Smoothing factor for plastic potential; value 1.0 is recommended
Char. length (RC)			ON/OFF	Enforced characteristic length flag for reinforced concrete
	$l_c^{RC}$	[m]	$> 0$	Characteristic length for reinforced concrete
Algorithmic setting			ON/OFF	Enforced using of secant stiffness instead of consistent tangent

Window 6-1

Window 6-2: Creep properties

ZSoil®

Parameter	Unit	Range	Description
Creep version		iEC:2008, EC:2008 (edition 2020) <sub>i</sub>	EC:2008 (edition 2020) highly recommended
$A$	[1/MPa]		$A = A_1 = \phi_{RH} \beta(f_{cm})/E$ (see EC2)
$B$	[day]		$B = \beta_H$ (see EC2)

Initial age	[day]	> 0.5	Age of analyzed concrete
Equivalent time flag		iON,OFF <sub>i</sub>	Flag whether to use temperature adjusted time
$\frac{Q}{R}$	[K]	4000	Ratio between activation energy and universal gas constant
$T_{ref}$	[C]	20	Reference temperature
$s$	[-]	0.38	Strength evolution parameter (EC2)
$t_{28}$	[day]	28.0	Time of 28 days in formula for $\beta_{cc}$ (EC2)
$n$	[-]	0.5	Exponent in expression for stiffness modulus (applied to $\beta_{cc}$ ) (EC2)

Window 6-2

**Remarks:**

1. In case of reinforced concrete structures modeled mainly with aid of shell elements, effects like strong strain localization do not usually occur; therefore scaling softening law is not needed; enforcing user defined characteristic length, independent on the element size, is the easiest trick to obtain mesh independent results (see Jofriet benchmark)
2. In case of regular problems one may use consistent tangent stiffness matrix in nonlinear FE computations; however, for problems in which significant strain localization effects may occur (especially when continuum elements are used instead of shells) using any form of tangent stiffness may lead to early failure of iterative schemes; the same effect may be observed when cracks open and then close again
3. In case when large finite elements are used some problems may arise from so-called snap backs; in these cases one may reduce strength value (usually tensile one) to reduce energy dissipation and sudden strength drop



# Chapter 7

## Benchmarks

### 7.1 Gopalaratnam and Shah monotonic and cyclic uniaxial tensile tests (1985)

Files: CPDM-UNIAX-TENS-GOP.inp, CPDM-UNIAX-TENS-CYCLIC-GOP.inp

Comparison of the experimental and numerical prediction of the  $\sigma - \varepsilon$  curves in the uniaxial (monotonic and cyclic) tensile tests (after Gopalaratnam and Shah) is the aim of this benchmark. This test is run with a single B8 element of size 82.6 mm x 82.6 mm x 82.6 mm[4] using displacement driven loading program. The test setup is shown in the following figure. Imposed displacements in X-direction are set at nodes 2,3,6 and 7.

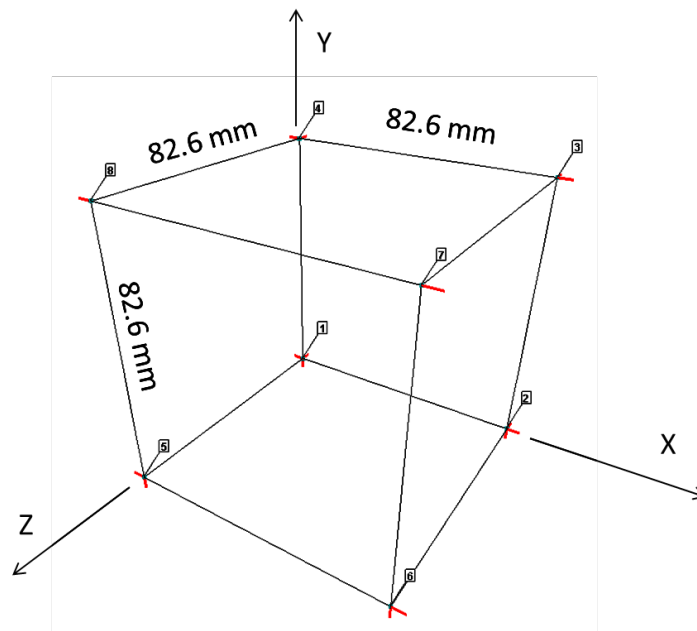


Figure 7.1: Uniaxial tensile test: mesh and boundary conditions

Material properties (after Lee and Fenves, 1998) are summarized in the table below. It should be mentioned that all parameters with the \* are not meaningful in the considered test.

Group	Subgroup	Parameter	Unit	Value
Elastic		$E$	[MPa]	31000
		$\nu$	[-]	0.18
Nonlinear	Compression	$\underline{f}_c$	[MPa]	27.6*
		$\underline{f}_{co}/\underline{f}_c$	[-]	0.4*
		$\underline{f}_{cbo}/\underline{f}_{co}$	[-]	1.16*
		$\underline{\sigma}_{c,D}/\underline{f}_c$	[-]	0.4*
		$\tilde{\sigma}_c/\underline{f}_c$	[MPa]	1.0*
		$\underline{D}_c$	[-]	0.4*
		$\underline{G}_c$	[MN/m]	$5.69 \cdot 10^{-3}$ *
		Calibration	[-]	Preserve $\underline{G}_c$ & $\tilde{D}_c$ *
	Tension	$\varepsilon_{c1}$	[-]	unused
		$\underline{f}_t$	[MPa]	3.48
		$\tilde{\sigma}_t/\underline{f}_t$	[-]	0.5
		$\underline{D}_t$	[-]	0.5
		$\underline{G}_t$	[MN/m]	$4 \cdot 10^{-5}$
		$s$	[-]	0.2*
	Dilatancy	Type		Constant
		$\underline{\sigma}_{c,dil}/\underline{f}_c$	[-]	0.4
		$\alpha_p$	[-]	0.20
		$\alpha_{po}$	[-]	0.20
		$\alpha_d$	[-]	1.0

The resulting  $\sigma_1 - \varepsilon_1$  curves for monotonic and cyclic tests are shown in the next two figures.

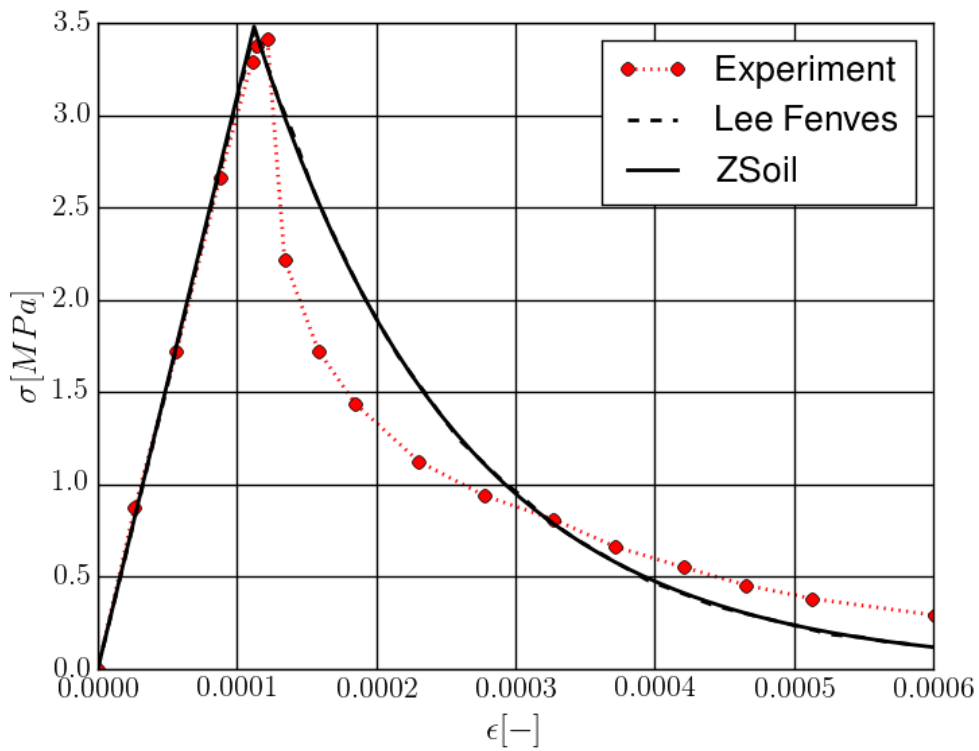


Figure 7.2: Uniaxial monotonic tensile test: comparizon of  $\sigma_1 - \varepsilon_1$  curves

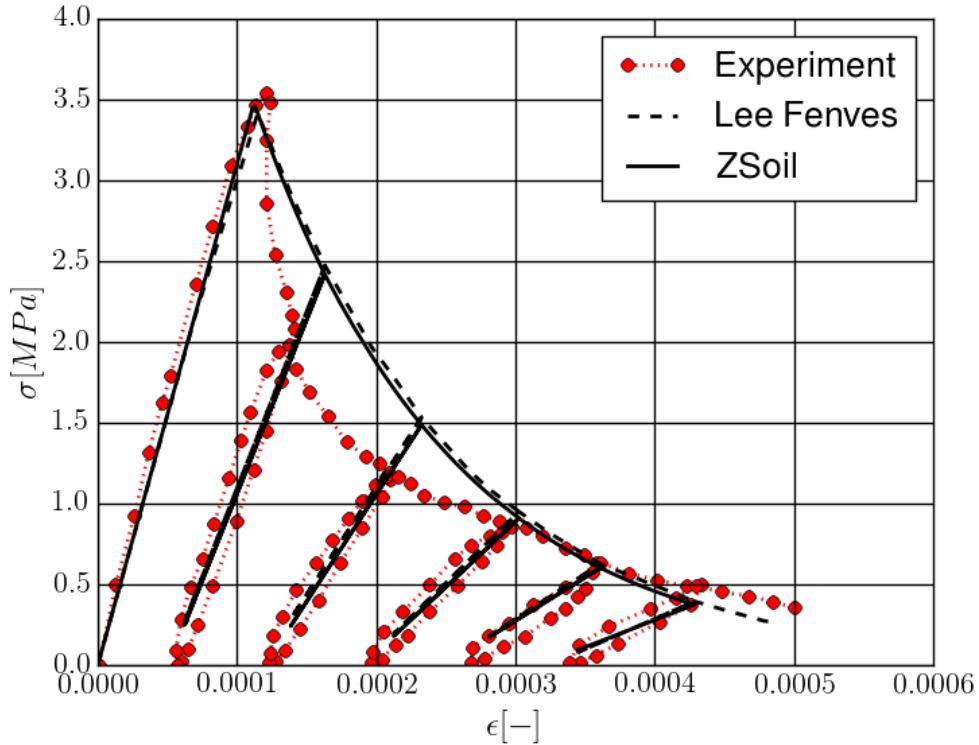


Figure 7.3: Uniaxial cyclic tensile test: comparizon of  $\sigma_1 - \varepsilon_1$  curves

## 7.2 Karsan and Jirsa monotonic and cyclic uniaxial compression tests (1969)

In this benchmark both the monotonic and cyclic uniaxial compression tests (after Karsan and Jirsa) are reproduced with aid of the plastic damage model. These tests are run with a single B8 element of size 82.6 mm x 82.6 mm x 82.6 mm [4] using displacement driven loading program. The test setup is shown in the following figure.

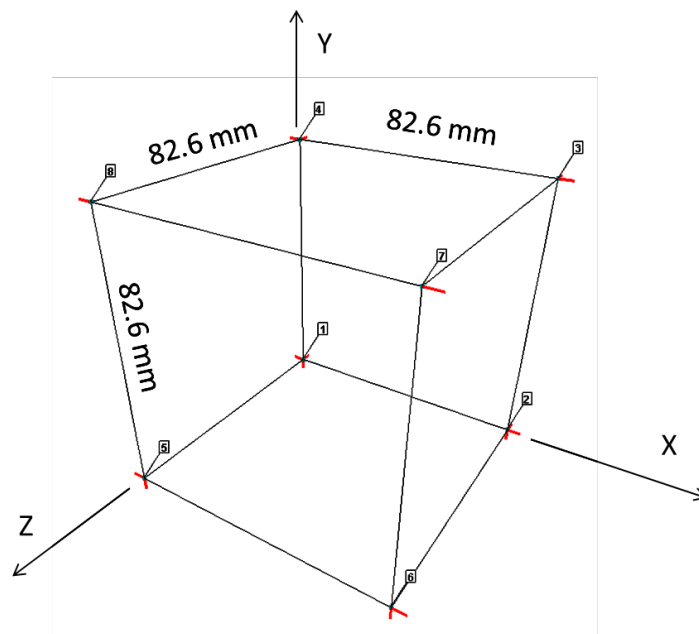


Figure 7.4: Uniaxial compression test: mesh and boundary conditions

Material properties (after Lee and Fenves, 1998) are summarized in the table below. It should be mentioned that all parameters with the \* are not meaningful in the considered test. Value of the parameter  $\underline{f}_{co}/\underline{f}_c$  ( $\underline{f}_{co}/\underline{f}_c = \underline{\sigma}_{c,dil}/\underline{f}_c = \underline{\sigma}_{c,D}/\underline{f}_c$  in the original formulation by Lee and Fenves) is not given in the article therefore it is assumed as  $\underline{f}_{co}/\underline{f}_c = 0.62$ .

Group	Subgroup	Parameter	Unit	Value
Elastic		$E$	[MPa]	31000
		$\nu$	[-]	0.18
Nonlinear	Compression	$\underline{f}_c$	[MPa]	27.6
		$\underline{f}_{co}/\underline{f}_c$	[-]	0.62
		$\underline{f}_{cbo}/\underline{f}_{co}$	[-]	1.16
		$\underline{\sigma}_{c,D}/\underline{f}_c$	[-]	0.62
		$\tilde{\sigma}_c/\underline{f}_c$	[-]	1.0
		$\bar{D}_c$	[-]	0.4
		$G_c$	[MN/m]	$5.69 \cdot 10^{-3}$
		Calibration	[-]	Preserve $G_c$ & $\bar{D}_c$
	Tension	$\varepsilon_{c1}$	[-]	unused
		$f_t$	[MPa]	3.48*
		$\tilde{\sigma}_t/f_t$	[-]	0.5*

7.2. KARSAN AND JIRSA MONOTONIC AND CYCLIC UNIAXIAL COMPRESSION TESTS (1969)

		$\tilde{D}_t$	[-]	0.5*
		$G_t$	[MN/m]	$4 \cdot 10^{-5}$ *
		$s$	[-]	0.2
	Dilatancy	Type		Constant
		$\sigma_{c,dil}/\underline{f}_c$	[-]	0.62
		$\alpha_p$	[-]	0.20
		$\alpha_{po}$	[-]	0.20
		$\alpha_d$	[-]	1.0

The resulting  $\sigma_1 - \varepsilon_1$  curves are shown in the next two figures.

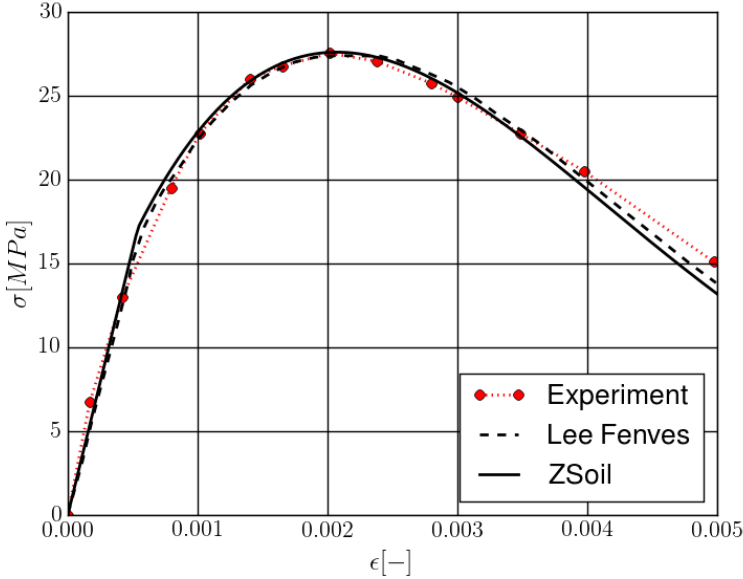


Figure 7.5: Uniaxial compression test: comparizon of  $\underline{\sigma}_1 - \underline{\epsilon}_1$  curves for monotonic compression test

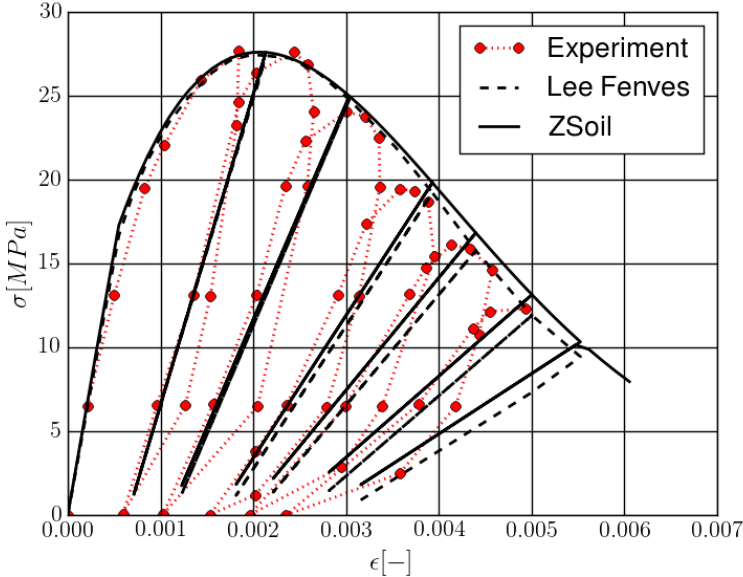


Figure 7.6: Uniaxial compression test: comparizon of  $\underline{\sigma}_1 - \underline{\epsilon}_1$  curves for cyclic uniaxial compression test

### 7.3 Kupfer's tests

Files: CPDM-Kupfer-1-0.inp, CPDM-Kupfer-1-0\_52.inp,  
 CPDM-Kupfer-1-0\_226.inp, CPDM-Kupfer-1-1.inp,  
 CPDM-Kupfer-1-t-0\_052.inp

In this benchmark the monotonic biaxial compression-compression and compression-tension tests (after Kupfer) are reproduced with aid of the plastic damage model. These tests are run with a 2x2 B8 elements of size 100.0 mm x 100.0 mm x 50.0 mm each (as in [4]) using spherical arc-length displacement control driver (node A is used to control displacements). To avoid nonuniform deformations all nodes in face A have same Z-displacement as node A (using periodic BC option). The test setup is shown in the following figure. Five tests are run for different  $q_1/q_2$  ratios i.e.  $q_1/q_2 = -1/0$  (uniaxial compression),  $q_1/q_2 = -1/-1$  (biaxial compression),  $q_1/q_2 = -1/-0.52$ ,  $q_1/q_2 = -1/-0.226$ ,  $q_1/q_2 = -1/+0.052$  (compression-tension).

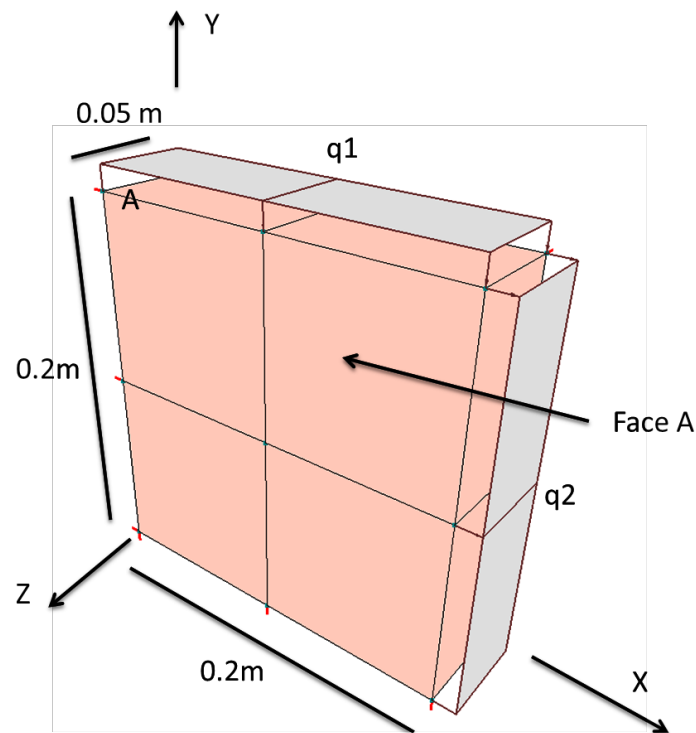


Figure 7.7: Kupfer tests: mesh and boundary conditions

Material properties, that were not given in the cited article, are summarized in the table below.

Group	Subgroup	Parameter	Unit	Value
Elastic		$E$	[MPa]	33000
		$\nu$	[-]	0.20
Nonlinear	Compression	$f_c$	[MPa]	32.4
		$f_{co}/f_c$	[-]	0.4
		$f_{cbo}/f_{co}$	[-]	1.15

Tension	$\frac{\sigma_{c,D}}{f_c}$	[-]	0.5
	$\frac{\tilde{\sigma}_c}{f_c}$	[-]	1.0
	$\tilde{D}_c$	[-]	0.44
	$G_c$	[MN/m]	$4.5 \cdot 10^{-3}$
	Calibration	[-]	Preserve $G_c$ & $\tilde{D}_c$
	$f_t$	[MPa]	3.24
	$\tilde{\sigma}_t/f_t$	[-]	0.5
	$\tilde{D}_t$	[-]	0.5
	$G_t$	[MN/m]	$1.5 \cdot 10^{-4}$
	Dilatancy	$s$	[-]
Type			Variable
$\frac{\sigma_{c,dil}}{f_c}$		[-]	0.8
$\alpha_p$		[-]	0.34
$\alpha_{po}$		[-]	0.20
$\alpha_d$		[-]	1.0

The resulting stress-strain diagrams are shown in the following figures

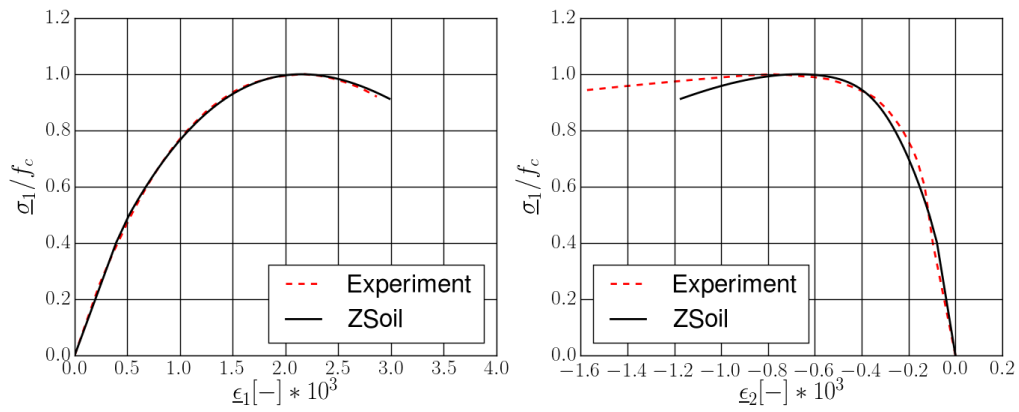


Figure 7.8:  $q_1/q_2 = -1/0$ :  $\sigma_1 - \varepsilon_1$  (left) and  $\sigma_1 - \varepsilon_2$  (right) diagrams

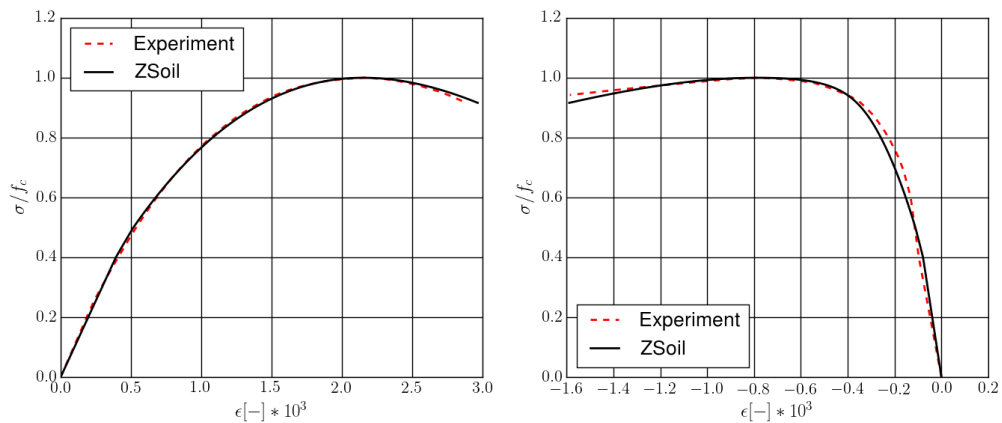
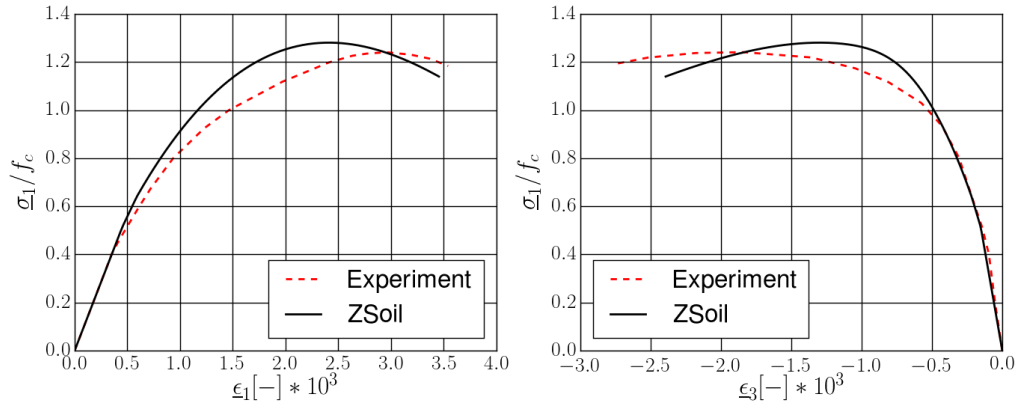
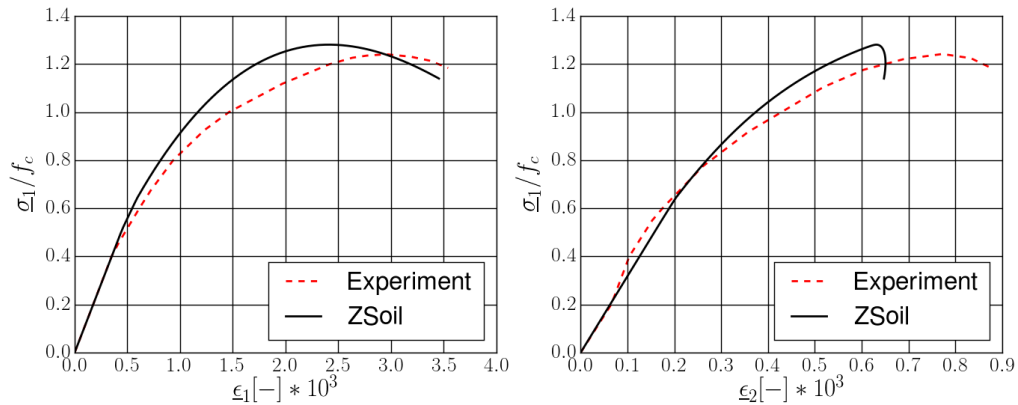
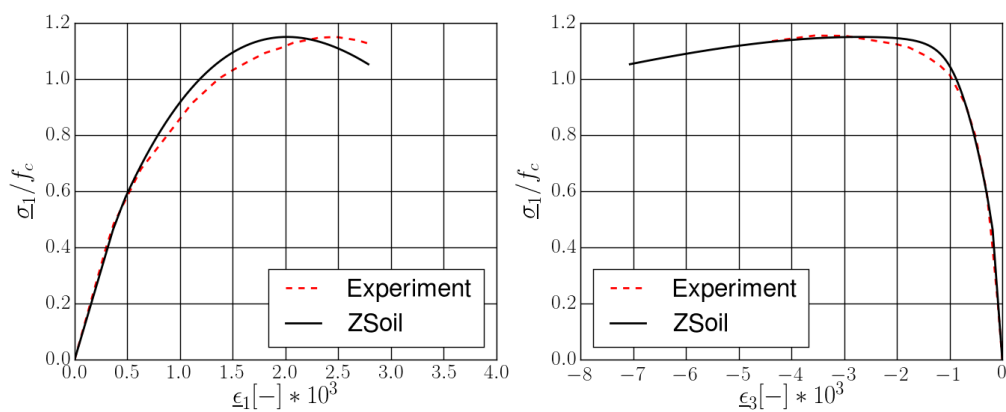


Figure 7.9:  $q_1/q_2 = -1/0$ :  $\sigma_1 - \varepsilon_1$  (left) and  $\sigma_1 - \varepsilon_2$  (right) diagrams for  $\alpha_p = 0.5$

Figure 7.10:  $q_1/q_2 = -1/-0.52$ :  $\sigma_1 - \epsilon_1$  (left) and  $\sigma_1 - \epsilon_3$  (right) diagramsFigure 7.11:  $q_1/q_2 = -1/-0.52$ :  $\sigma_1 - \epsilon_1$  (left) and  $\sigma_1 - \epsilon_2$  (right) diagramsFigure 7.12:  $q_1/q_2 = -1/-1$ :  $\sigma_1 - \epsilon_1$  (left) and  $\sigma_1 - \epsilon_3$  (right) diagrams

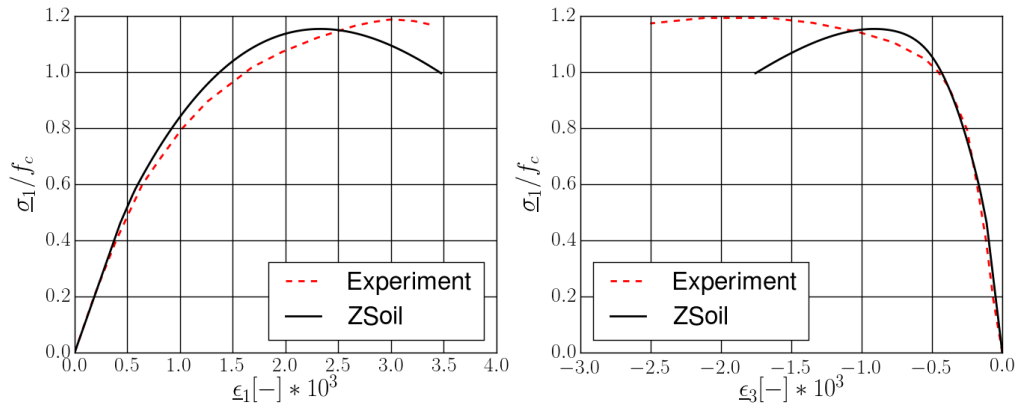


Figure 7.13:  $q_1/q_2 = -1 / -0.226$ :  $\sigma_1 - \epsilon_1$  (left) and  $\sigma_1 - \epsilon_3$  (right) diagrams

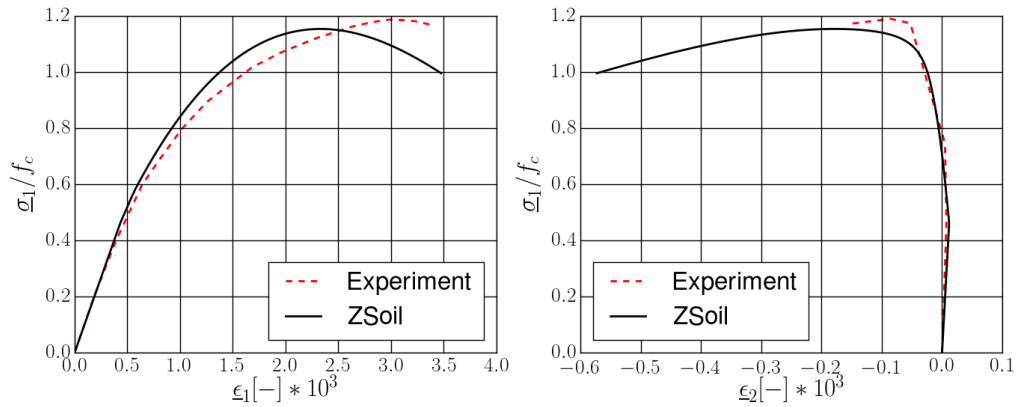


Figure 7.14:  $q_1/q_2 = -1 / -0.226$ :  $\sigma_1 - \epsilon_1$  (left) and  $\sigma_1 - \epsilon_2$  (right) diagrams

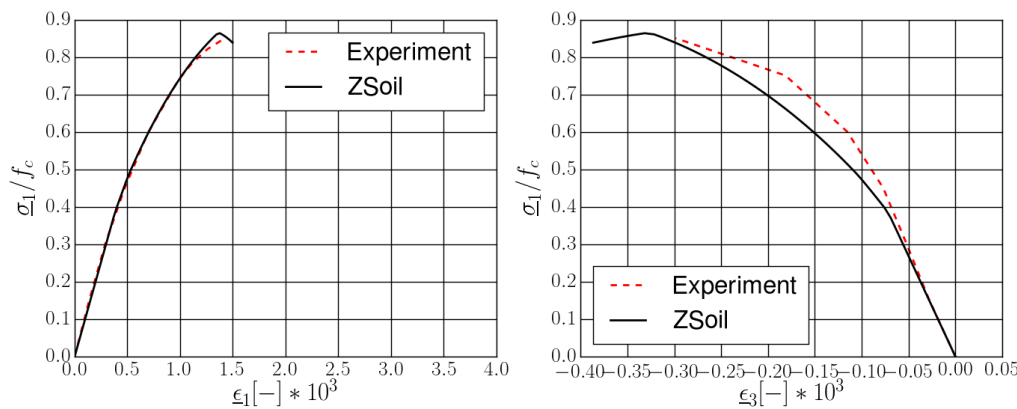


Figure 7.15:  $q_1/q_2 = -1 / +0.052$ :  $\sigma_1 - \epsilon_1$  (left) and  $\sigma_1 - \epsilon_3$  (right) diagrams

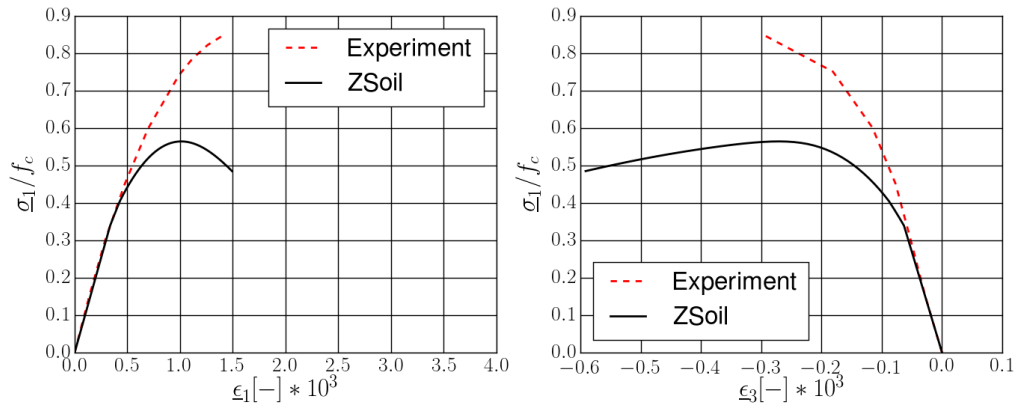


Figure 7.16:  $q_1/q_2 = -1/ + 0.052$ :  $\sigma_1 - \epsilon_1$  (left) and  $\sigma_1 - \epsilon_3$  (right) diagrams without modification of the yield condition (reference model,  $\rho = 0.0$  )

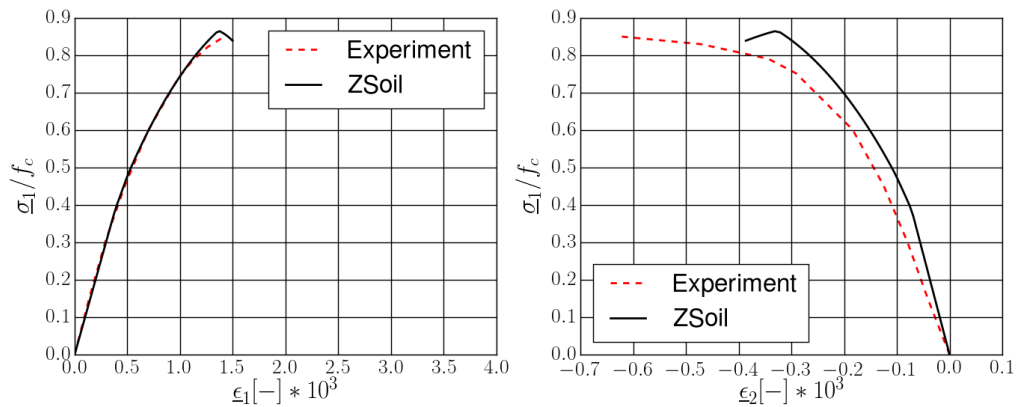


Figure 7.17:  $q_1/q_2 = -1/ + 0.052$ :  $\sigma_1 - \epsilon_1$  (left) and  $\sigma_1 - \epsilon_2$  (right) diagrams

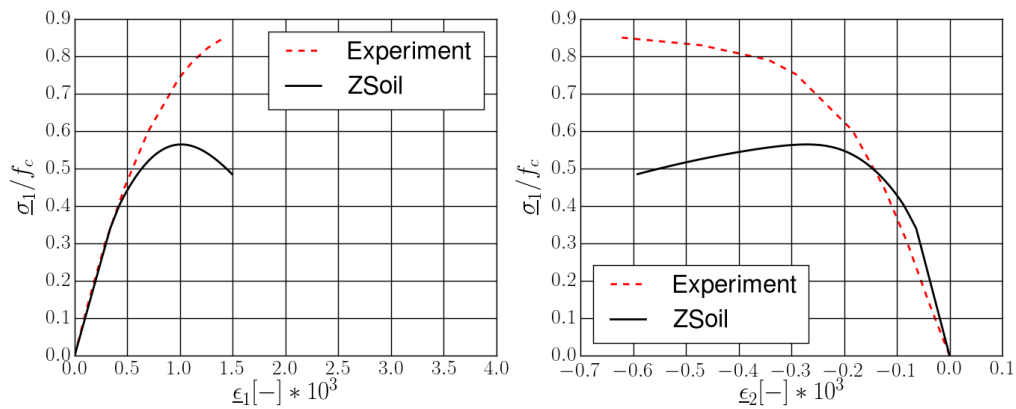


Figure 7.18:  $q_1/q_2 = -1/ + 0.052$ :  $\sigma_1 - \epsilon_1$  (left) and  $\sigma_1 - \epsilon_2$  (right) diagrams without modification of the yield condition (reference model,  $\rho = 0.0$  )

## 7.4 Three point bending test

### Files:Malvar-Warren-ps.inp

The three point bending test for plain concrete, carried out experimentally by Malvar and Warren [6], is analyzed in this section. Geometry of the notched specimen, mesh and boundary conditions used in the test, run as a plane-strain problem, are shown in the following figure. The element adjacent to the fixed node in the right bottom point is modeled as elastic to cancel local plastic effects. A displacement driven loading program, with the maximum assumed deflection of 5mm is used with 50 equal steps.

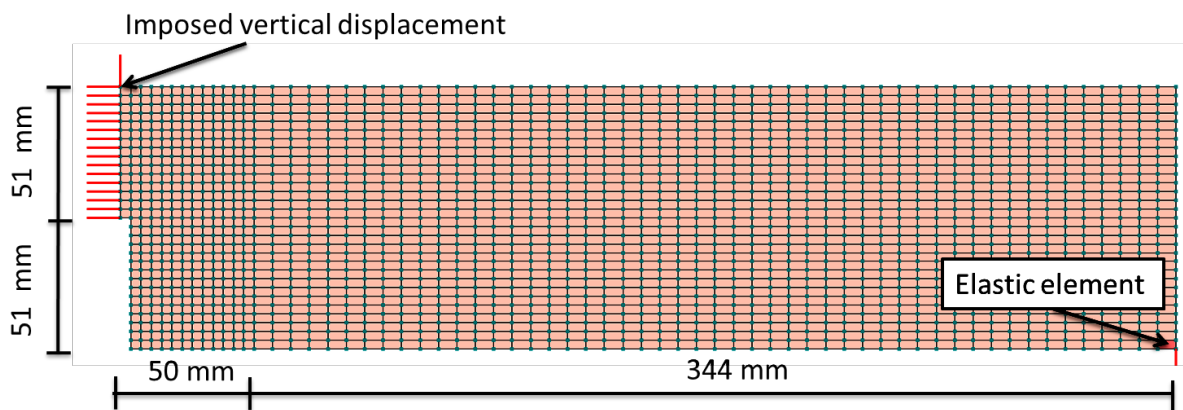


Figure 7.19: Three point bending test: geometry, mesh and boundary conditions

Material properties are summarized in the following table.

Parameter	Unit	Value
$E$	[MPa]	21700
$\nu$	[-]	0.20
$\underline{f}_c$	[MPa]	29.0
$\underline{f}_{co}/\underline{f}_c$	[-]	0.6
$\underline{f}_{cbo}/\underline{f}_{co}$	[-]	1.16
$\underline{\sigma}_{c,D}/\underline{f}_c$	[-]	0.5
$\tilde{\sigma}_c/\underline{f}_c$	[-]	1.0
$\bar{D}_c$	[-]	0.5
$G_c$	[MN/m]	$4.5 \cdot 10^{-3}$
$f_t$	[MPa]	3.1
$\tilde{\sigma}_t/f_t$	[-]	0.5
$\bar{D}_t$	[-]	0.55
$G_t$	[MN/m]	$0.65 \cdot 10^{-4}$
$s$	[-]	0.2
Dilatancy		Constant
$\underline{\sigma}_{c,dil}/\underline{f}_c$	[-]	0.6
$\alpha_p$	[-]	-
$\alpha_{po}$	[-]	0.20
$\alpha_d$	[-]	1.0

Comparison of the experimental and numerical force-deflection diagrams is shown in Fig.7.20. The ZSoil prediction quite well matches the experimental curve reported by Malvar and Warren. The peak is predicted at same deflection as in the experiment and a small overshoot is visible just after the peak. This effect can be explained by a specific form of the softening described by an exponential function. It has to be mentioned that Lee and Fenves obtained their result by diminishing the tensile strength from 3.1 MPa to 2.4 MPa and tensile fracture energy from 70 [N/m] to 30 [N/m]. This effect can only be explained by the fact that their elements did not suffer from severe locking phenomenon.

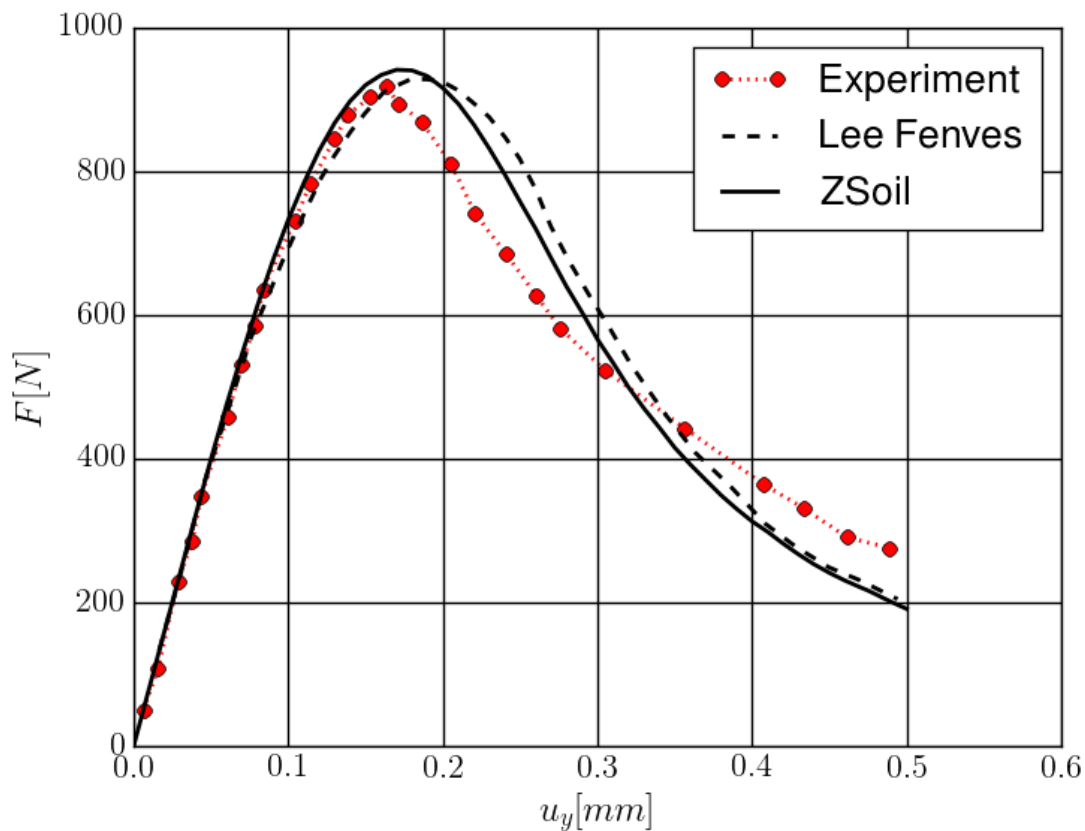


Figure 7.20: Three point bending test: comparison of experimental and numerical force-deflection diagrams

## 7.5 RC slab under point loading

**Files:** Jofriet-3x3.inp, Jofriet-6x6.inp, Jofriet-12x12.inp

A square reinforced concrete slab with dimensions [2] 91.44 cm × 91.44 cm, 4.45cm thick, simply supported at four corners, and loaded by a concentrated force at the center, is analyzed here (see Fig.7.21). Due to dual symmetry only one quarter is discretized. The slab is reinforced by an orthogonal reinforcement with density  $\rho = 0.85\%$  same in both directions. The averaged effective depth of the cross section is equal to 3.33 cm (to simplify the analysis

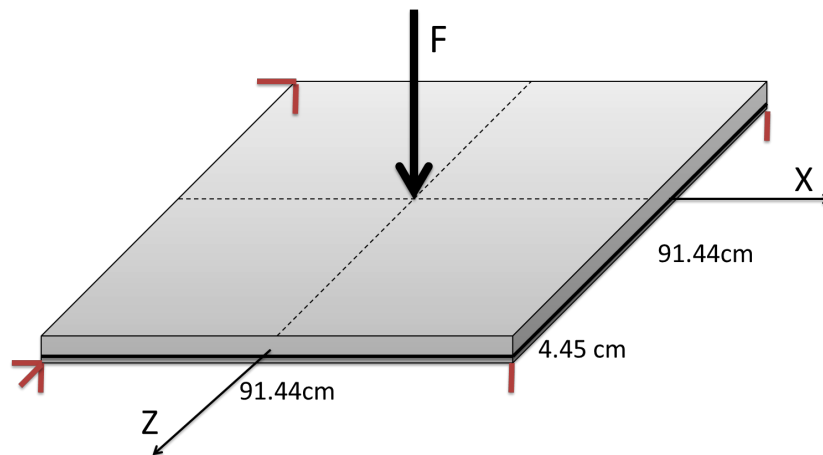


Figure 7.21: RC slab: geometry and boundary conditions

both reinforcement layers are placed at 1.12 cm from the bottom fibers). It is very important to cancel membrane forces by proper setting of boundary conditions. Material properties for concrete, taken from publication published by Krätzig et al. [3], are as follows:

Material properties are summarized in the following table.

Parameter	Unit	Value
$E$	[MPa]	28613
$\nu$	[-]	0.15
$f_c$	[MPa]	37.92
$\frac{f_{co}}{f_c}$	[-]	0.6
$\frac{f_{cbo}}{f_{co}}$	[-]	1.16
$\frac{\sigma_{c,D}}{f_c}$	[-]	0.5
$\frac{\tilde{\sigma}_c}{f_c}$	[-]	1.0
$\tilde{D}_c$	[-]	0.5
$G_c$	[MN/m]	$3.0 \cdot 10^{-3}$
$f_t$	[MPa]	2.91
$\frac{\tilde{\sigma}_t}{f_t}$	[-]	0.5
$\tilde{D}_t$	[-]	0.7
$G_t$	[MN/m]	$1.5 \cdot 10^{-4}$
$s$	[-]	0.2
Dilatancy		Constant
$\frac{\sigma_{c,dil}}{f_c}$	[-]	0.6
$\alpha_p$	[-]	-
$\alpha_{po}$	[-]	0.20
$\alpha_d$	[-]	1.0
$l_c^{RC}$	[m]	0.13

Steel is modeled with an elastic-plastic model characterized by Young modulus  $E_s = 201300$  MPa and strength  $f_y = 345.4$  MPa.

Comparison of the experimental and numerical force-displacement diagrams are shown in Fig. 7.22, 7.23. A typical mismatch between the model and experiment is observed at deflections

in range  $1 \div 2$  mm. It can be reduced by diminishing the tensile strength up to  $f_t = 2.3$  MPa (see Krätzig et. al). Better prediction can be obtained for fixed value of the characteristic length  $l_c^{RC} = 0.13$  m.

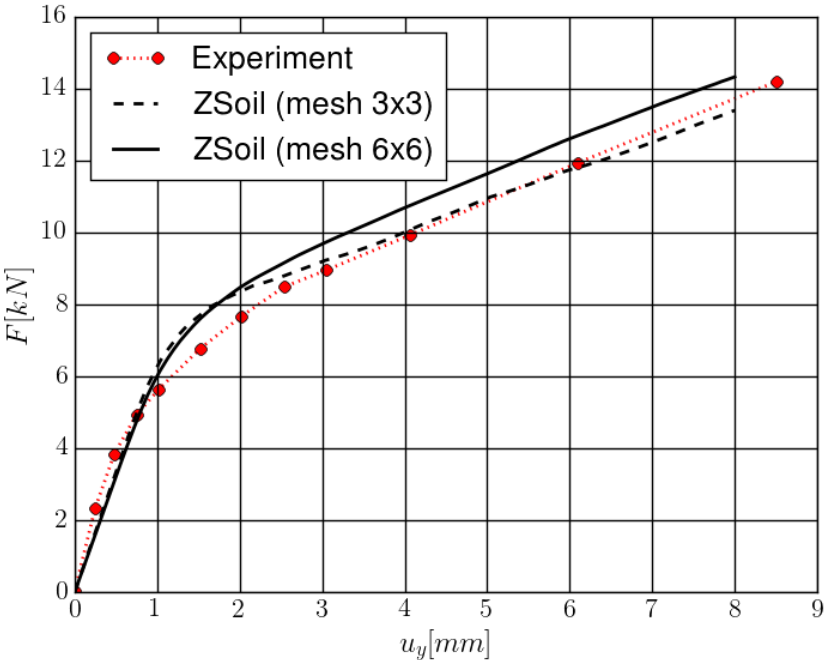


Figure 7.22: RC slab: comparizon of experimental and numerical force-deflection diagrams ( $l_c = h^e$ )

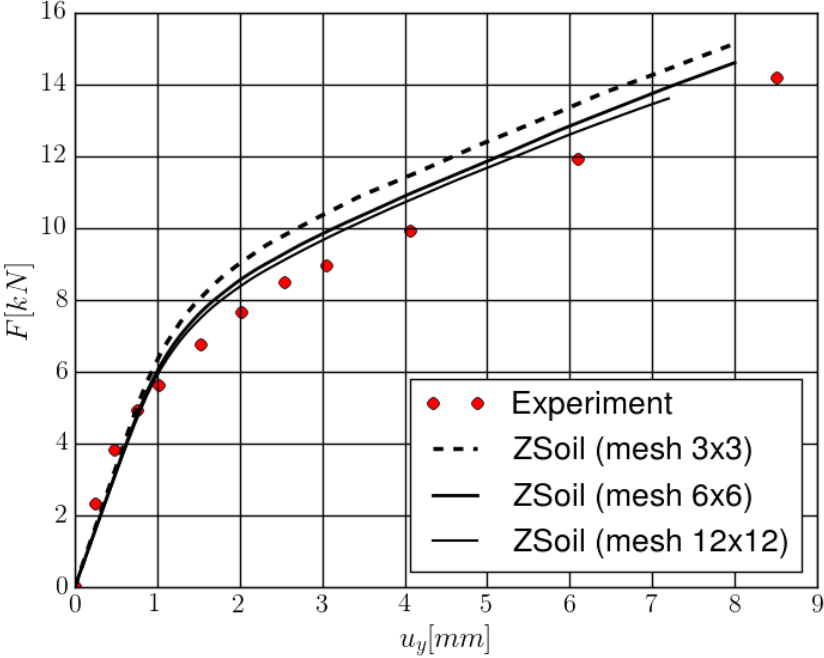


Figure 7.23: RC slab: comparizon of experimental and numerical force-deflection diagrams for fixed value of characteristic length  $l_c^{RC} = 0.13$  m

## 7.6 Creep in monotonic compression test

Files:

CPDM-aging-creep-cont-2D-to-2days.inp,  
CPDM-aging-creep-cont-2D-to-2days-ex.inp,  
CPDM-aging-creep-cont-2D-to-3days.inp,  
CPDM-aging-creep-cont-2D-to-3days-ex.inp,  
CPDM-aging-creep-cont-2D-to-7days.inp,  
CPDM-aging-creep-cont-2D-to-7days-ex.inp,  
CPDM-aging-creep-cont-2D-to-14days.inp,  
CPDM-aging-creep-cont-2D-to-14days-ex.inp,  
CPDM-aging-creep-cont-2D-to-28days.inp,  
CPDM-aging-creep-cont-2D-to-28days-ex.inp,  
CPDM-aging-creep-cont-2D-to-90days.inp  
CPDM-aging-creep-cont-2D-to-90days-ex.inp  
CPDM-aging-creep-shell-to-2-days  
CPDM-aging-creep-shell-to-2-days-ex

In all data files with added extension -ex a new edition 2020 of creep module is used. The test setup is shown in the following figure.

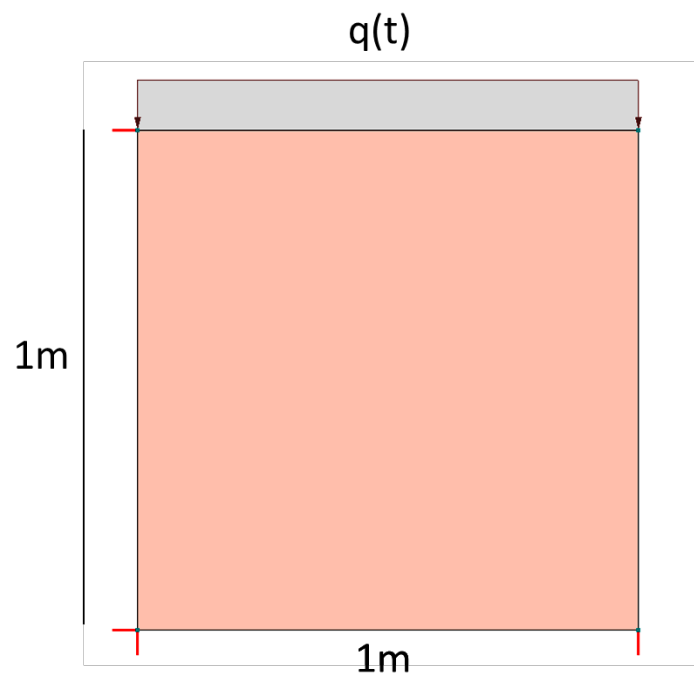


Figure 7.24: Test setup for creep in uniaxial compression test

Elastic and nonlinear material properties are the same as in the Kupfer test (7.3) except Poisson value that is equal to zero here. Creep properties are summarized in the following table

Parameter	Unit	Value
$A$	[1/MPa]	$9 \cdot 10^{-5}$
$B$	[day]	500
Initial age ( $t_o$ )	[day]	2/3/7/14/28/90
Equivalent time flag		OFF
$\frac{Q}{R}$	[K]	unused
$T_{ref}$	[C]	unused
$s$	[-]	0.38
$t_{28}$	[day]	28
$n$	[-]	0.5

Load time function associated with the uniform loading is defined as

time [days]	LTF (t)
0	0
0.01	0.1

The resulting displacement time histories are shown in the figure below. Perfect agreement between theory and EC2 creep model is observed for both creep module editions.

Same result is obtained when layered Q4-MITC shell element is used (here only  $t_o = 2$  days is considered)

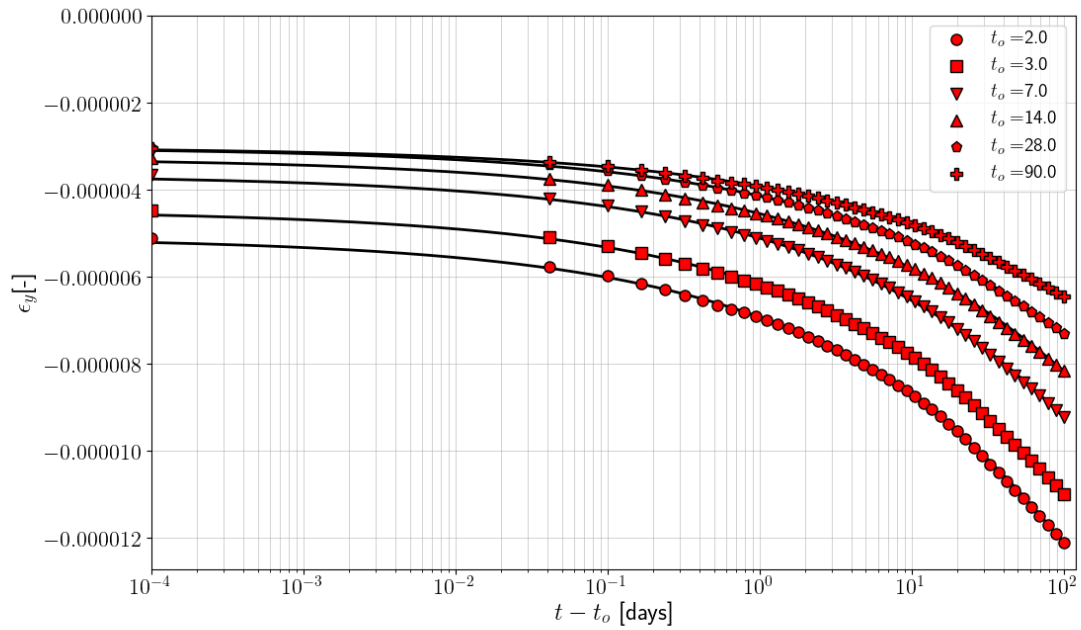


Figure 7.25: Evolution of  $\varepsilon_y(t)$  for different loading times (analytical solution is drawn with solid line)

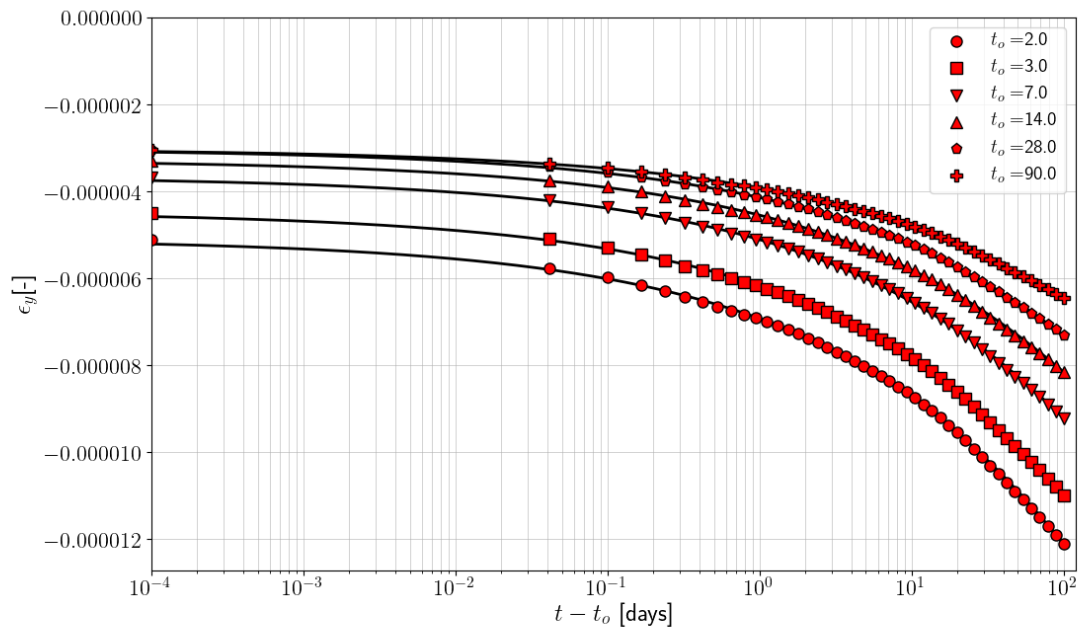


Figure 7.26: Evolution of  $\varepsilon_y(t)$  for different loading times (Edition 2020)(analytical solution is drawn with solid line)

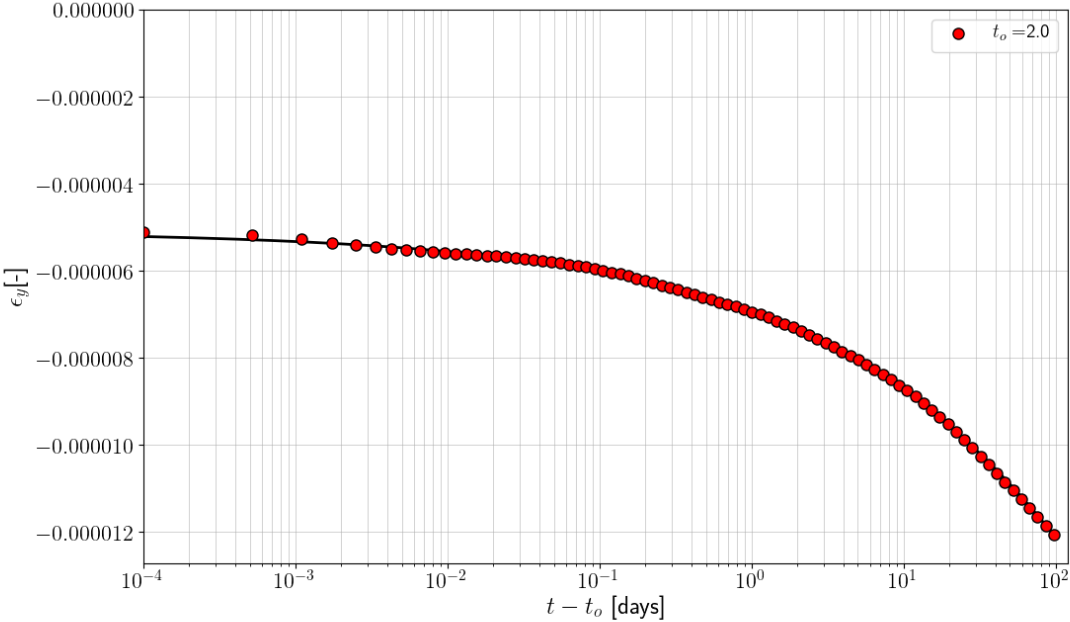


Figure 7.27: Evolution of  $\varepsilon_y(t)$  for  $t_o = 2$  [days] (shell element is used here)(analytical solution is drawn with solid line)

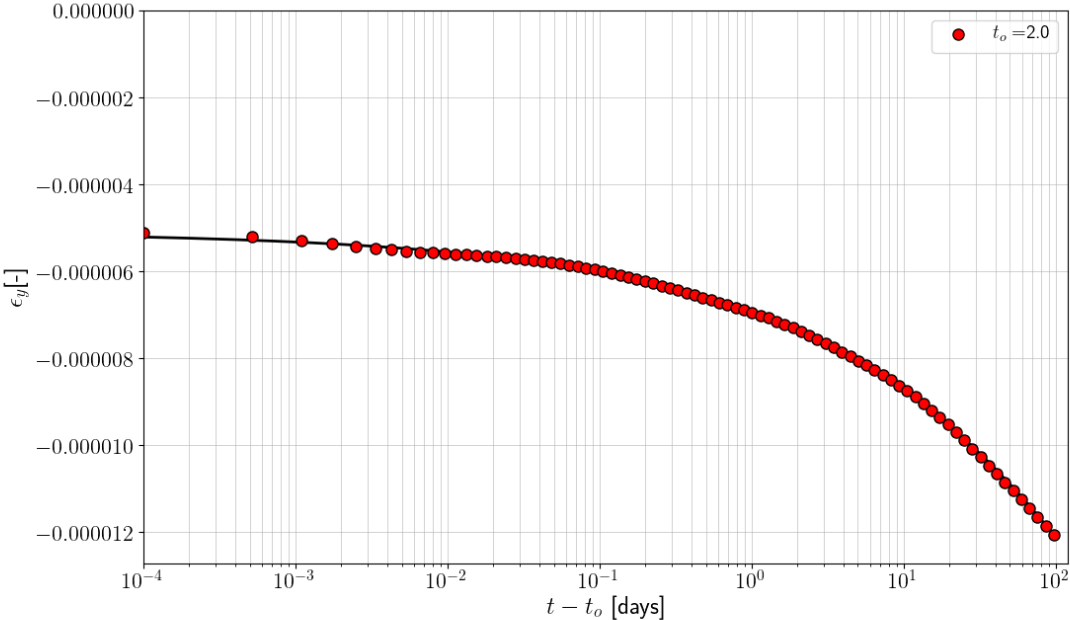


Figure 7.28: Evolution of  $\varepsilon_y(t)$  for  $t_o = 2$  [days] (shell element is used here)(Edition 2020)(analytical solution is drawn with solid line)

## 7.7 Creep under variable loading conditions

Files:

**CPDM-aging-creep-cont-2D-superp.inp,**  
**CPDM-aging-creep-cont-2D-superp-ex.inp**

Showing the effect of creep superposition for a single element compression test is the aim of this benchmark. The test setup and material data is exactly the same as in the benchmark shown in section 7.6 except the age of the concrete that is equal to  $t_o = 90$  [days] here. The element is loaded at time  $t = 0$  (time at beginning of the analysis while age of concrete is equal to 90 days) with  $q(t = 0) = 0.1 \text{ MN/m}^2$ . At time  $t = 5$  days  $q(t = 5) = 0.2 \text{ MN/m}^2$ . Comparizon of the analytical and numerical solutions is shown in the following figures.

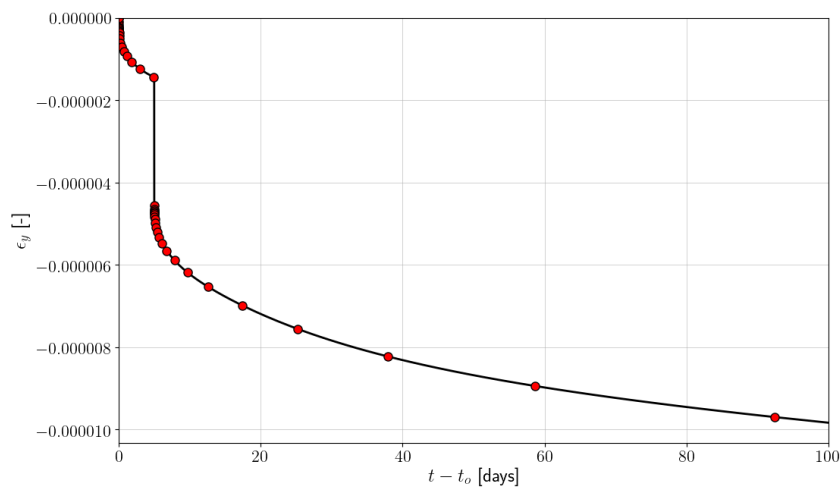


Figure 7.29: Evolution of  $\varepsilon_y(t)$

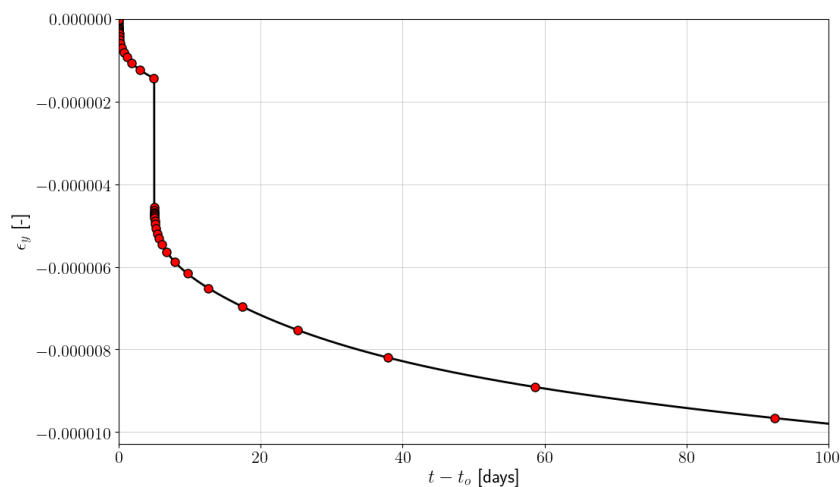


Figure 7.30: Evolution of  $\varepsilon_y(t)$  (Edition 2020)

## 7.8 Creep under variable loading conditions at early stage of maturing

Files:

CPDM-aging-creep-cont-2D-superp-to-7.inp,

CPDM-aging-creep-cont-2D-superp-to-7-ex.inp

Showing the effect of creep superposition for a single element compression test and comparison of the previous and the Edition 2020 of the creep module is the aim of this benchmark. The test setup and material data is exactly the same as in the benchmark shown in section 7.6 except the age of the concrete that is equal to  $t_o = 7$  [days] here. The complex loading and finally unloading program is shown in the figure below. Comparison of the time history of vertical strain  $\varepsilon_y(t)$  for the previous and the new Edition 2020 is shown in the fig.7.32. It is well visible that the previous implementation was generating larger creep strains in the loading phase but also in the unloading one.

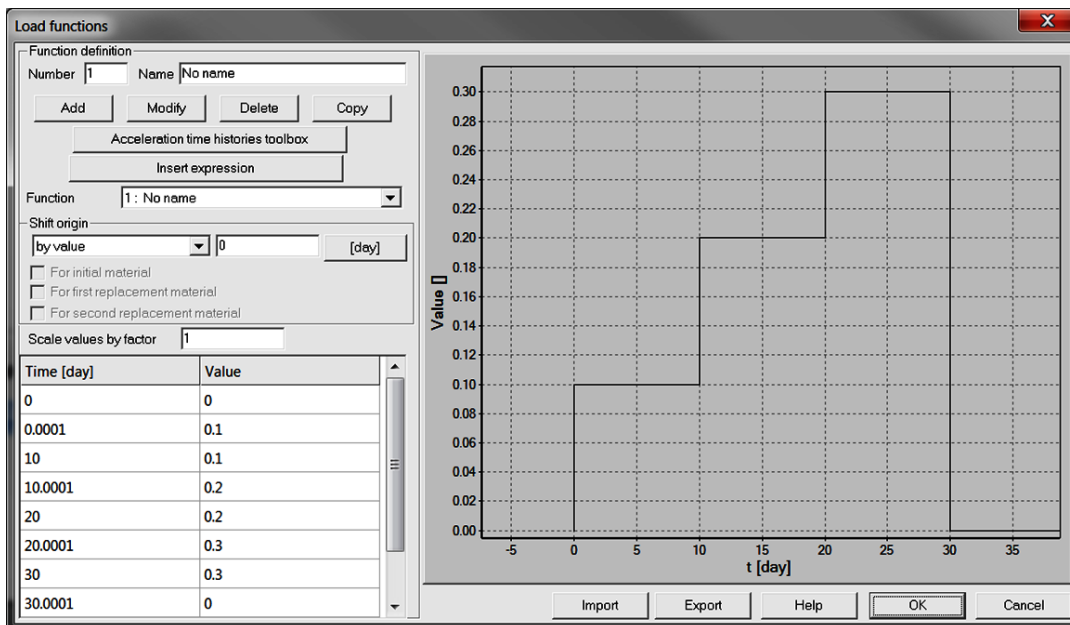


Figure 7.31: Loading program  $q(t)$

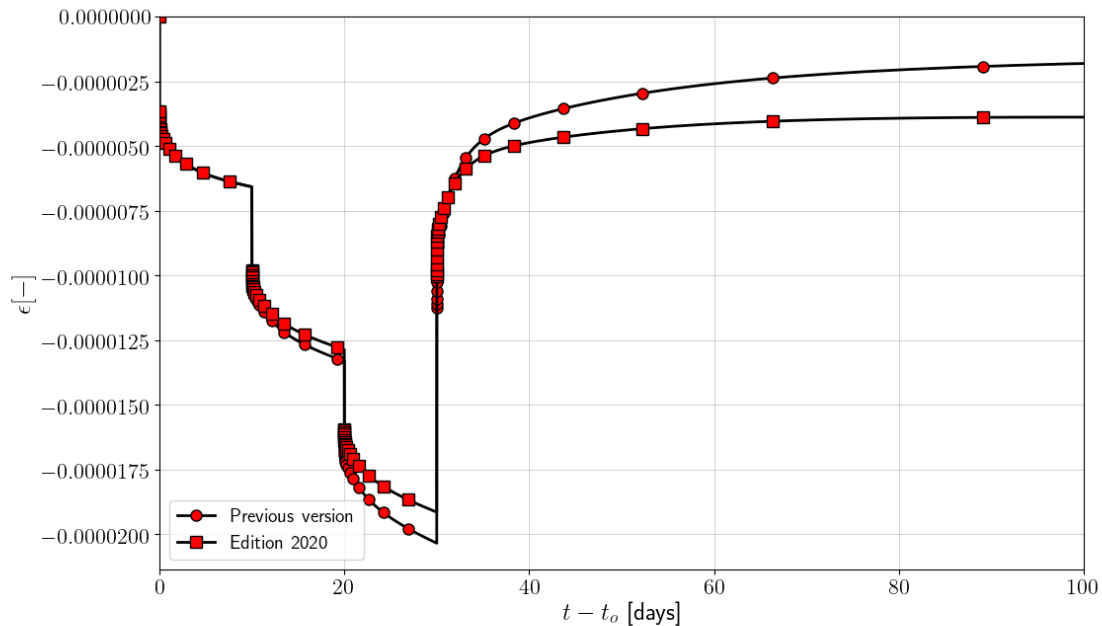


Figure 7.32: Evolution of  $\epsilon_y(t)$ ; comparizon of the previous vs Edition 2020 creep implementations

## 7.9 Nonlinear monotonic creep compression test

### Files:

**CPDM-aging-creep-cont-2D-0\_4fc.inp,**

**CPDM-aging-creep-cont-2D-0\_6fc.inp,**

**CPDM-aging-creep-cont-2D-0\_8fc.inp**

The test setup and material data is exactly the same as in the benchmark shown in section 7.6 except the age of the concrete that is equal to  $t_o = 28$  [days] here and the applied stress level. Three stress levels  $\sigma_c/f_c(28)$  are analyzed ie.  $\sigma_c/f_c(28) = 0.4, 0.6, 0.8$  Comparizon of the analytical (EC2) vs numerical predictions is shown in the fig.7.33. It is obvious that the compressive creep amplification proposed in the EC2 cannot be matched by the current creep module although effect of amplification is qualitatively present. For practical cases and expected stress level one may tune creep parameters to achieve a good match between the model and EC2 standard.

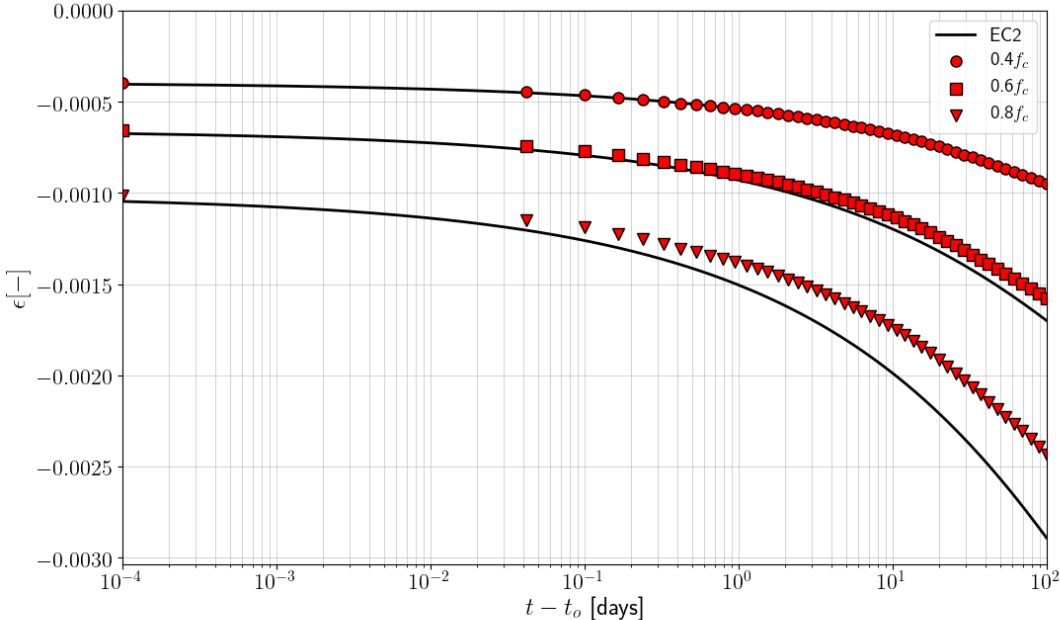


Figure 7.33: Evolution of  $\varepsilon_y(t)$  for three stress levels  $\sigma_c/f_c(28) = 0.4, 0.6, 0.8$

# Bibliography

- [1] P. Havlásek. *Creep and Shrinkage of Concrete Subjected to Variable Environmental Conditions*. PhD thesis, Czech Technical University in Prague, 2014.
- [2] J. C. Jofriet and M. McNeice. Finite element analysis of reinforced concrete slabs. *J. Struct. Division (ASCE)*, 97(3ST):785–806, 1971.
- [3] W. B. Krätzig and R. Pölling. An elasto-plastic damage model for reinforced concrete with minimum number of material parameters. *Computers and Structures*, 82:1201–1215, 2004.
- [4] J. Lee and G. Fenves. Plastic-damage model for cyclic loading of concrete structures. *Journal of Engineering Mechanics*, 124:892–900, 1998.
- [5] J. Lee and G. Fenves. A return-mapping algorithm for plastic-damage models: 3-D and plane stress formulation. *IJNME*, 50:487–506, 2001.
- [6] L. Malvar and G. Warren. Fracture energy for three-point-bend tests on single-edge-notched beams. *Experimental Mechanics*, 45:266–272, 1988.
- [7] O. Omidí and V. Lotfi. Continuum large cracking in a rate-dependent plastic-damage model for cyclic-loaded concrete structures. *IJNMG*, 37:1363–1390, 2012.